Journal of Medicinal Chemistry

Article

Fluorinated Chaperone—#-Cyclodextrin Formulations for #-Glucocerebrosidase Activity Enhancement in Neuronopathic Gaucher Disease

M. Isabel Garcia-Moreno, Mario de la Mata, Elena Matilde Sánchez-Fernández, Juan M. Benito, Antonio J. Díaz-Quintana, Santos Fustero, Eiji Nanba, Katsumi Higaki, José A Sánchez Alcázar, José Manuel García Fernández, and Carmen Ortiz Mellet

J. Med. Chem., **Just Accepted Manuscript** • DOI: 10.1021/acs.jmedchem.6b01550 • Publication Date (Web): 07 Feb 2017

ACS Publications

Journal of Medicinal Chemistry is published by the American Chemical Society. 1155 Sixteenth Street N.W., Washington, DC 20036

Fluorinated Chaperone—β-Cyclodextrin Formulations for β-Glucocerebrosidase Activity Enhancement in Neuronopathic Gaucher Disease

M. Isabel García-Moreno,[†,#] Mario de la Mata,[‡,#] Elena M. Sánchez-Fernández,[†] Juan M. Benito,[§] Antonio Díaz-Quintana,[§] Santos Fustero,[‖] Eiji Nanba,[⊥] Katsumi Higaki,[⊥] José A. Sánchez-Alcázar,*[‡] José M. García Fernández,*[§] Carmen Ortiz Mellet*[†]*

[†]Department of Organic Chemistry, Faculty of Chemistry, University of Sevilla, c/ Profesor García González 1, 41011 Sevilla, Spain

[‡]Centro Andaluz de Biología del Desarrollo (CABD), CSIC – Universidad Pablo de Olavide, and Centro de Investigación Biomédica en Red: Enfermedades Raras (CIBERER), Instituto de Salud Carlos III, Carretera de Utrera Km 1, 41013 Sevilla, Spain

[§]Instituto de Investigaciones Químicas (IIQ), CSIC – Universidad de Sevilla, Avda. Américo Vespucio 49, E-41092 Sevilla, Spain

[⊥]Division of Functional Genomics, Research Center for Bioscience and Technology, Tottori University, 86 Nishi-cho, Yonago 683-8503, Japan

[‖]Departamento de Química Orgánica, Universidad de Valencia, 46100 Burjassot, Spain, and Laboratorio de Moléculas Orgánicas, Centro de Investigación Príncipe Felipe, 46012 Valencia, Spain

ABSTRACT: Amphiphilic glycomimetics encompassing a rigid, undistortable *nor*-tropane skeleton based on 1,6-anhydro-L-idonojirimycin and a polyfluorinated antenna, when formulated as the corresponding inclusion complexes with β-cyclodextrin (βCD), have been shown to behave as pharmacological chaperones (PCs) that efficiently rescue lysosomal β-glucocerebrosidase mutants associated to the neuronopathic variants of Gaucher disease (GD), including the highly refractory L444P/L444P and L444P/P415R single nucleotide polymorphs, in patient fibroblasts. The body of work here presented includes the design criteria for the PC prototype, the synthesis of a series of candidates, the characterization of the PC:βCD complexes, the determination of the selectivity profiles towards a panel of commercial and human lysosomal glycosidases, the evaluation of the chaperoning activity in type 1 (non-neuronopathic), 2 (acute neuronopathic) and 3 (adult neuronopathic) GD fibroblasts, the confirmation of the rescuing mechanism by immunolabeling and the analysis of the PC:GCase binding mode by docking experiments.

Introduction

Lysosomal acid β-glucosidase (β-glucocerebrosidase, GCase; EC 3.2.1.45) catalyzes the hydrolysis of the β-glycopyranosyl linkage in glucosylceramide (GlcCer) and glucosylsphingosine (GlcSph, psychosine) downstream in glycosphingolipid metabolism, producing the free sugar and lipid components.[1-3] Dysfunction of GCase results in progressive accumulation of undigested GlcCer and GlcSph in lysosomes of macrophage cells and visceral organs,[4,5] which is the underlying pathological manifestation of Gaucher disease (GD), the

lysosomal storage disorder (LSD) with the highest prevalence (1 in 57,000 live births in the general population; 1 in 1,000 in Ashkenazi Jews).[6,7] For operational purposes, GD is subdivided in three clinical types depending on the age of onset and the severity of the symptoms. Type 1 GD (OMIM# 230800) is non-neuropathic and benefits from the availability of enzyme replacement therapy (ERT, i.e., supplementation with a recombinant GCase enzyme)[8] and substrate reduction therapy (SRT, i.e., administration of inhibitors of substrate biosynthesis).[9,10] In contrast, type 2 and 3 GD (OMIM# 230900, and 231000, respectively), which accounts for 5-10% of patients worldwide, course with neurological deterioration and remain orphan.[11]

The origin of GCase dysfunction causing GD is diverse. However, abnormal protein folding during biosynthesis in the endoplasmic reticulum (ER) and subsequent ER-associated degradation (ERAD) is often observed.[12] Ironically, many of the disease-associated mutant GCase forms are catalytically competent and able to process putative substrates at rates compatible with normal life, provided the unfolded protein response (UPR) leading to ERAD is bypassed.[13-15] The use of pharmacological chaperones (PCs) to rescue the endogenous mutant enzyme by stabilizing the folding conformation and restoring trafficking represents, therefore, an interesting and, in principle, more general therapeutic option.[16-18] Various classes of synthetic compounds have been studied as PCs for GD (Figure 1), including glycomimetics[19] of the iminosugar (e.g. **1**, **2**),[20,21] carbasugar (e.g. **3**)[22] and aminocyclitol (e.g. **4**)[23] families, amino sugar derivatives (e.g. **5**, **6**)[24-26] and non-carbohydrate-related compounds identified after high-throughput screening in drug repositioning programs (e.g. **7**, **8**).[27,28] With few exceptions,[29] most of these compounds proved active in enhancing GCase activity only in type 1 GD fibroblast cells, i.e., hosting the N370S mutation in homo- or heterozygosis. Aiming at addressing the neuronopathic forms of the disease, our laboratories developed a new family of PC candidates

based on very versatile amphiphilic sp^2-iminosugar frameworks related to the natural alkaloids nojirimycin and castanospermine (e.g. **9**, **10**).[30-32] The GCase rescuing mechanism was demonstrated in fibroblasts[33] and in dopaminergic neurons (differentiated from induced pluripotent stem cells) of patients suffering from type 2 and 3 GD[34] The chaperoning effect was, however, restricted to mutations located in the catalytic domain of the enzyme, which do not include the L444P homozygotes having the highest prevalence among neuropathic GD patients.

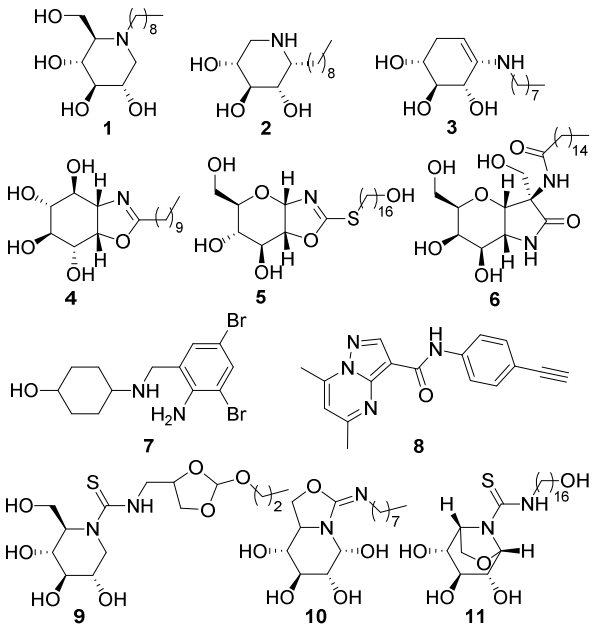

Figure 1. Structures of representative iminosugar (**1**, **2**), carbasugar (**3**), aminocyclitol (**4**), amino sugar (**5**, **6**), non-glycomimetic (**7**, **8**) and sp^2-iminosugar (**9**-**11**) derivatives with pharmacological chaperone activity in Gaucher cells.

Inspection of X-ray structural data of complexes between GCase and chaperones with either monocyclic[20] or condensed bicyclic cores[35,36] revealed that the sugar-like portion of the PC is distorted upon binding to the enzyme, the six-membered ring adopting an envelope or skew-boat conformation instead of the thermodynamically more stable chair conformation present in the unbound state. This induced-fit binding mechanism probably demands a very low

conformational effort from the protein side, confining the refolding potential of the PC to the regions near the catalytic site. We envisaged that chaperones encompassing an undistortable glycone moiety mimicking the glucose portion of GlcCer will instead force the protein to better adjust its conformation in order to form a tight-bound chaperone:GCase complex, thereby propagating the correct folding and stabilizing effects more efficiently beyond the catalytic domain. As a proof of concept, *nor*-tropane (calystegine)-based amphiphilic sp^2-iminosugars (e.g. **11**) were developed[37,38] and found to exhibit unprecedented L444P/L444P GCase activity enhancing capabilities *ex-vivo*.[39,40] As for the natural calystegine alkaloids, the bridged bicyclic core imparts selectivity towards GCase among lysosomal enzymes.[41,42] Notably, replacing the basic amino groups by a neutral thiourea functionality with strong hydrogen-bond donor capabilities does not annul the glycosidase inhibitory/chaperoning potential, which is in agreement with observations in the nojirimycin glycomimetic series, and improves membrane-crossing abilities.[30,43] However, the incorporation of a hydrophobic *N'*-substituent is required to achieve biologically useful enzyme affinities.[44] Interestingly, the presence of the ω-hydroxyhexadecyl aglycone segment in compound **11** was particularly beneficial, which was ascribed to the interplay of hydrophobic interactions with amino acids at the entrance of the catalytic site of GCase and a long range hydrogen bond interaction (see SI, Figure S1).[39] We now conceived that replacement of the terminal segment in the hydrocarbon tail by a polyfluorinated fragment might further favor complex stability and GCase rescuing capabilities by providing additional contacts with protein surfaces, a strategy that has proven very successful in medicinal chemistry schemes.[45,46]

Fluoroalkylation of iminosugars has been found to increase affinity against some complementary glycosidases[47-49] and is also expected to enhance biological membrane crossing

capabilities, including across the blood-brain barrier (BBB),[50] which is critical in PC therapy addressing neuronopathic pathologies. The high tendency of amphiphilic polyfluorocompounds to form colloidal aggregates might represent a serious limitation for pharmaceutical use, decreasing the effective concentration of the free drug and thwarting a medically relevant result.[51] Moreover, aggregation may lead to multivalent presentations of the PC motif, which may profoundly affect the affinity and selectivity profile towards protein partners.[52,53] To avert these risks, here we capitalize on the high avidity of polyfluorinated amphiphiles towards the cavity of β-cyclodextrin (βCD)[54] to prevent PC micellization (Figure 2).[55] βCD is a commercially available biocompatible cyclooligosaccharide broadly used in the pharmaceutical industry to enhance the bioavailability of drugs by increasing their water solubility, avoiding aggregation and/or improving drug permeability. Interestingly, βCD increases the membrane-crossing capabilities of hydrophobic drugs hosted in the cavity, including penetration across the BBB,[56] by making the single molecule drug available at the surface where it partitions into the membrane without disrupting the lipid layers of the barrier.[57] The design and synthesis of the fluorinated pharmacological chaperone prototypes, the characterization of the corresponding inclusion complexes with βCD, the enzyme inhibition properties of the free and complexed chaperones and the GCase activity enhancement in GD cells hosting different mutations associated to neuronopathic variants of the disease are reported.

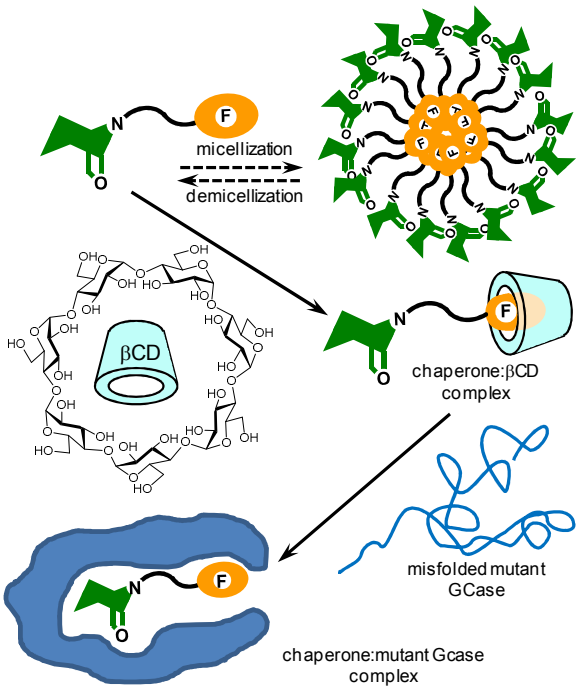

Figure 2. Schematic representation of the proposed strategy for Gaucher disease chaperone therapy based on fluorinated sp^2-iminosugars with an undistortable 1,6-anhydro-L-idonojirimycin core equipped with fluorinated aglycones. The high avidity of the fluorocarbon moiety towards the cavity of β-cyclodextrin should prevent micellization and favor the transfer of the chaperone to the active site of disease-causative misfolded glucocerebrosidase. Since the protein cannot distort the chaperone, it will be forced to adopt a properly folded conformation, which will be stabilized by additional interactions with the fluorinated segment. The properly folded enzyme will escape degradation at the ER and trafficking to the lysosome will be restored.

Results and Discussion

Design criteria and synthesis. Replacement of a hydrocarbon segment by a polyfluorocarbon moiety in the aglycone fragment of the chaperone implies an increase in chain rigidity that may hamper the capacity of the molecule to properly adapt to complementary surface regions in the protein, especially when considering allosteric interactions.[58] To prevent such eventuality, we

chose to insert a polymethylene portion between the undistortable *nor*-tropane aglycone core and the terminal fluorinated part (Figure 2). This molecular design is compatible with a modular synthetic approach involving: (i) an L-idose precursor of the glycomimetic scaffold that will provide the desired all-*trans*-equatorial glucose-like stereochemistry at the key triol segment, (ii) a bifunctional alkylidene derivative incorporating simultaneously an isothiocyanate group to generate the thiourea functionality, thereby imparting the sp^2-iminosugar feature, and a *tert*-butoxycarbonyl (Boc)-protected amino group for additional conjugation, and (iii) a linear polyfluoroalkyl carboxylic acid suitable for chemoselective amide coupling with an amine-armed chaperone intermediate (Figure 3).

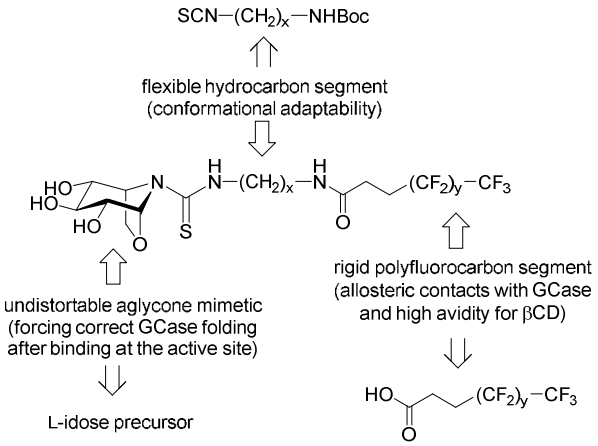

Figure 3. General structure of the proposed chaperone prototype and retrosynthetic scheme with indication of the key building blocks.

A divergent synthetic scheme was implemented that allows generating molecular diversity with a relatively low synthetic cost. Starting from 5-amino-5-deoxy-1,2-isopropylidene-L-idofuranose (**13**), readily accessible from commercial D-glucuronolactone,[59] thiourea coupling reaction with the bifunctional derivatives **13** and **14**, with four and nine methylene groups, respectively, afforded the corresponding adducts **15** and **16**. Acid-treatment promotes concomitant hydrolysis of the isopropylidene and Boc protecting groups. Upon neutralization

with Amberlite® IRA 68 (OH^-) ion-exchange resin, intramolecular nucleophilic addition of the N-thiourea atom to the masked aldehyde group of the monosaccharide takes place, resulting in the furanose→piperidine rearrangement. The resulting reducing sp^2-iminosugar spontaneously undergoes intramolecular glycosylation involving the primary hydroxyl group to give, in a single step and in excellent yield, the bicyclic 1,6-anhydro-L-idonojirimycin (AIJ) skeleton of **17** and **18** already armed with a terminal amino group. After peptide conjugation with the carboxylic acid derivatives **19** and **20**, a library of four AIJ derivatives, namely **21**-**24**, endowed with aglycone-like moieties of different lengths and combinations of hydrocarbon and polyfluorocarbon segments was generated.

Scheme 1. Synthesis of the 1,6-Anhydro-L-Idonojirimycin Incorporating Fluorinated Aglycone Substituents 21-24.

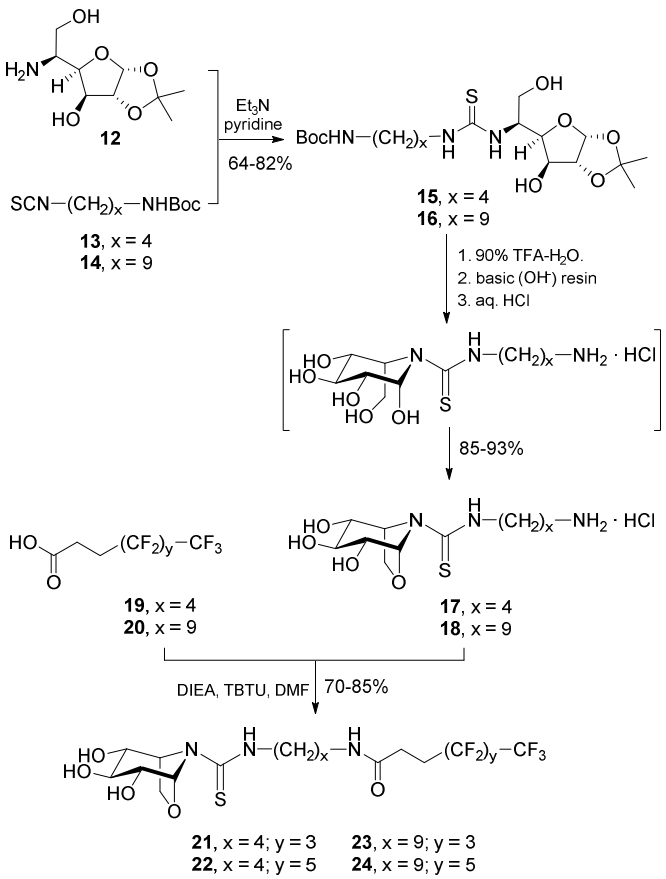

Aggregation and Inclusion Complex Formation with β-Cyclodextrin. The critical micellar concentrations (CMC) of compounds **21**-**24** were measured by the pyrene method.[60] Briefly, the fluorescence intensity of the pyrene molecule experiences an abrupt increase when confined to the hydrophobic environment of a micelle as compared with bulk water, which can be detected in a classical fluorimetric titration experiment. CMC values of 393 μM (for **21**), 31.6 μM (for **22**), 37.5 μM (for **23**) and 15.0 μM (for **24**) were thus obtained (see SI, Figures S19 to S22). Except for **21**, these values are in the range of the concentrations encountered for optimal chaperone activity in cell cultures of patients suffering from lysosomal storage disorders with brain involvement, and in all cases are much lower than the chaperone concentrations needed to have a medically relevant result *in vivo* (over 1 mM).[61] We, therefore, prepared and characterized the corresponding inclusion complexes with βCD prior to biological evaluation.

The water solubility of all four fluorinated chaperones **21**-**24** was highly increased in the presence of βCD; no aggregation was observed at equimolecular chaperone:host ratios of up to 1 mM. For comparison, α-cyclodextrin (αCD) was unable to promote any significant water solubility enhancement, supporting the fact that the inclusion of the polyflurocarbon moiety in the βCD cavity is responsible for this observation. NMR titration experiments conducted with derivatives **21** and **22**, sharing the tetramethylene segment, afforded binding isotherms fitting 1:1 PC:βCD complexes (i.e., one molecule of βCD encapsulates a single molecule of the fluorinated chaperone),[62] with association constant (K_a) values 7.5±0.7 $\cdot 10^3$ M^{-1} and 3.4±0.3 $\cdot 10^4$ M^{-1} (see Supporting Information, Figures S31 and S32). In the case of the homologs having the nonamethylene segment **23** and **24**, the low water solubility of the chaperone prevented a parallel thermodynamic study by NMR. Nevertheless, formation of the corresponding inclusion complexes was equally supported by ^{1}H NMR data in the presence of excess of βCD. Given that

the fluorinated moieties are identical in **21** or **23** and in **22** or **24**, similar K_a values and the same 1:1 complex stoichiometry would be expected. It is noteworthy that association constants of about 10^3-10^4 M^{-1} are in the optimal range for pharmaceutical formulations and warrant the efficient transfer of the chaperone from the inclusion complex to the target protein, for which the binding constant with sp^2-iminosugar substrate analogs is typically in the 10^6-10^7 range.[63]

Enzyme Inhibition Properties. In a preliminary assay, the inhibitory properties of compounds **21**-**24** and their corresponding 1:1 complexes with βCD were assessed against a panel of commercial glycosidases covering a variety of configurational and anomeric specificities, including bovine and almond β-glucosidase, yeast α-glucosidase and isomaltase, *Aspergillus niger* amyloglucosidase, *Escherichia coli* β-galactosidase, green coffee bean α-galactosidase, *Helix pomatia* β-mannosidase, and Jack bean α-mannosidase (Table 1). Strong competitive inhibition (inhibition constant, K_i, values in the low μM-to-nM range) was exclusively observed against the mammalian β-glucosidase enzyme. Compounds **21** and **22** additionally behaved as weak inhibitors of the plant isoenzyme (K_i >100 μM). In any case, the configurational and anomeric selectivity towards β-glucosidase was outstanding: no inhibition of any of the other glycosidases was observed at sp^2-iminosugar concentrations of up to 1 mM (uncomplexed) or 2 mM (βCD complexes).

Table 1. K_i Values (μM) for 21-24 and their 1:1 Complexes with βCD against Glycosidases.[a,b,c,d,e]

Enzyme	**21**	**21**:βCD	**22**	**22**:βCD	**23**	**23**:βCD	**24**	**24**:βCD
β-Glcase (bovine liver)	6.4 ±0.2	1.3±0.1	1.1±0.1	0.13±0.02	0.34±0.03	0.26	0.33±0.05	2.5±0.1
GCase (human, pH 5)	20.8± 0.7	4.5±0.1	90±4	1.4±0.3	80±5	8.2±0.5	32.6±0.6	7.2±0.3

GCcase (human, pH 7)	35±2	0.30 ±0.03	11.9±0.5	0.09±0.01	9.3±0.6	0.9±0.1	4.1±0.3	0.6±0.1

[a]Data are presented as mean±SD (n = 3). [b]Inhibition was competitive in all cases except for **24**:βCD against bovine liver β-glucosidase, which was mixed-type (uncompetitive component K'_i = 2.6±0.1 μM). [c]No inhibition was observed for any compound at 1 mM (free) or 2 mM concentration (βCD complexes) on baker's yeast isomaltase, *Aspergillus niger* amyloglucosidase, green coffee bean α-galactosidase, Jack bean α-mannosidase and *Helix pomatia* β-mannosidase. [d]No inhibition was observed for any compound at 200 μM on lysosomal α-glucosidase, α- and β-galactosidases, α- and β-mannosidases and hexosaminidase in cell lysates. [e]Control experiments using βCD at a 2 mM concentration in the absence of **21**-**24** showed no inhibition at all for any of the assayed enzymes.

Further assessment of the inhibition abilities of **21**-**24** against human lysosomal glycosidases in cell lysates (*in vitro* enzyme assay; see Experimental) confirmed the selectivity pattern previously observed for the commercial enzymes: whereas GCase was responsive to μM concentrations of the fluorinated sp^2-iminosugars (K_i values in the range of 20-90 μM at pH 5; 3-12 μM at pH 7), the activity of lysosomal α-glucosidase, α- and β-galactosidases, α- and β-mannosidases and hexosaminidase was not affected at concentrations of up to 200 μM. Interestingly, the corresponding complexes of **21**-**24** with βCD behaved as stronger inhibitors of GCase than the free compounds, with K_i values in the low μM range at pH 5 and in the nM range at pH 7, suggesting that the enzyme is sensitive to inhibitor aggregation and that demicellization through inclusion complex formation improves GCase binding affinity. This effect is particularly dramatic in the case of compound **22**, for which the co-formulation with βCD led to 66- (pH 5) and 126-fold (pH 7) enhancements in the inhibitory potency towards GCase (Table 1). The above-ten-fold lower K_i values at neutral pH (0.09 to 0.9 μM) as compared to acidic pH (1 to 7 μM) is generally considered as a positive feature for chaperone candidates: it means that the compound will bind stronger to GCase at the ER, where stabilization of the correct folding is required, than at the lysosome, where dissociation of the chaperone:GCase complex is necessary to allow substrate processing.

Chaperoning Capabilities of Fluorinated sp^2-Iminosugar:βCD Complexes in Gaucher Fibroblasts. The effects of the new fluorinated sp^2-iminosugars **21**-**24** and their inclusion complexes with βCD on GCase activity and cell viability were first investigated in healthy human fibroblasts. For that purpose, cells were cultured for 5 days in the absence and in the presence of various concentrations of the compounds, then lysed and the enzyme activity was determined using 4-methylumbelliferyl β-D-glucopyranoside as substrate. An enhancement in the measured GCase activity in the lysate indicates that larger amounts of the protein are present and that it is able to process the substrate. In this sense, it is worth mentioning that although GCase inhibition is generally considered a valuable indication for PC drug candidates, a higher inhibitory potential does not necessarily translate into a better performance as a PC. If displacement of the inhibitor from the enzyme:inhibitor complex is strongly disfavored, the enzyme would not be functional even though the compound may restore the proper folding and trafficking of mutant GCase variants.[64]

Compounds **21** and **23**, bearing a perfluorobutyl terminal moiety, had no significant effect neither on GCase activity nor on cell viability at concentrations of up to 100 μM (data not shown), neither in free form nor when complexed with βCD. However, the corresponding homologs **22** and **24**, with a perfluorohexyl moiety, decreased GCase activity by 30-50% at a concentration of 20 μM and induced a cell death of 45-75% at 100 μM when used in their uncomplexed form (see SI, Table S1). Both GCase inhibition and cell mortality were abolished when the compounds were formulated with βCD in the concentration window of interest, strongly suggesting that aggregation of the free fluorinated amphiphiles was responsible for these observations.

The fluorinated sp^2-iminosugar (**21**-**24**):βCD complexes, showing no aggregation-related adverse effects, were further evaluated with regard to the GCase activity enhancement in Gaucher fibroblasts from patients hosting the N370S/N370S, N370S/84GG (non-neuronopathic, type 1 GD), V230G/R296X, L444P/P415R (acute neuronopathic, type 2 GD), N188S/G183W or L444P/L444P mutations (neuronopathic, type 3 GD), following the aforementioned protocol for healthy fibroblasts (Table 2). The results, collectively presented in Figure 4, which represent mean values from three independent experiments, each carried out in triplicate, evidenced significant differences as a function of both the GD causative mutation and the chaperone formulation.

Table 2. Characteristics of the GCase variants assayed in this study.

GCase variant	Location	Severity	Responsiveness to PC therapy NN-DNJ (**1**) / ambroxol (**7**)[a]
N370S/N370S	Domain III	Type 1 GD	+ / +
N370S/84GG	Domain III	Type 1 GD	+ / +
V230G/R296X	Domain III	Type 2 GD	–[b] / +
L444P/P415R	Domain II	Type 2 GD	– / +[c]
N188S/G183W	Domain II	Type 3 GD	+ / +
L444P/L444P	Domain II	Type 3 GD	–[d] / +[c]

[a]The + and – signs indicate responsive and not responsive, respectively. [b]Responsive to the acid-sensitive sp^2-iminosugar **9**. [c]Medically useful activity enhancements are only reached at relatively high concentrations (>50 μM). [d]Responsive to calystegine-type sp^2-iminosugar **11**.

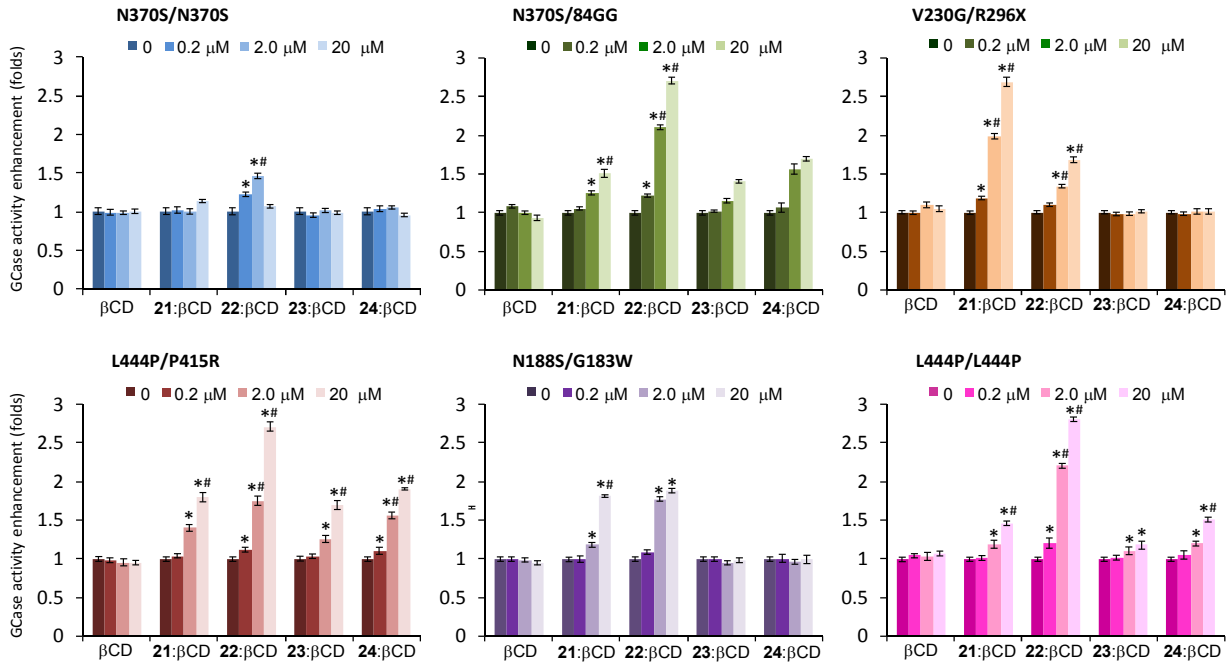

Figure 4. Chaperone activity of **21**-**24**:βCD complexes in cultured human fibroblasts of type 1 (N370S/N370S and N370S/84GG), type 2 (V230G/R296X and L444P/P415R), and type 3 (N188S/G183W) Gaucher patients. Each bar represents the mean±standard error (SEM) of 3 determinations each done in triplicate. Control experiments conducted with βCD in the absence of **21**-**24** showed no effect in GCase activity for any of the mutants. *$p < 0.05$, statistically different from the value of untreated samples. #$p < 0.05$, statistically different from the value obtained for the precedent ten-fold lower concentration of the PC:βCD complex.

The non-neuronopathic homozygous N370S mutation, the most prevalent in type 1 GD patients, was moderately responsive to treatment with **22**:βCD (1.5-fold GCase activity enhancement at a concentration of 2 μM), in line with results obtained with other sp^2-iminosugars[30,32] but considerably weaker when compared to other glycomimetic-type candidates.[19,21-23] The other three fluorinated sp^2-iminosugar formulations behaved very poor or were inactive as chaperones in the same cell assay. Indeed, structural and biochemical data

indicated that the protein is already correctly folded in N370S/N370S GD patients and that the mechanism by which some protonable competitive inhibitors increase the lysosomal levels of GCase is by reducing degradation by means of proteases within the lysosome, rather than by having an effect on protein folding and trafficking;[65] neutral sp^2-iminosugars are instead designed to assist folding at the ER but dissociate from the protein at the lysosome.[19] The second type 1 GD mutation evaluated in this study, namely N370S/84GG, was much more sensitive to chaperoning by the fluorinated sp^2-iminosugar:βCD complexes, with GCase activity enhancements with approx. 1.5- to 1.7-fold GCase activity enhancements for **21**:βCD, **23**:βCD and **24**:βCD and reaching 2.8-fold for **22**:βCD ad 20 μM.

The acute-neuronopathic (early onset) type 2 GD-associated mutations V230G/R296X and L444P/P415R are located in the catalytic and in the non-catalytic domain of GCase, namely domains III and II, respectively.[19,66] The first was previously found to respond only very modestly to sp^2-iminosugars with distortable cores,[64] unless equipped with a pH-sensitive mechanism ensuring full dissociation in the lysosome (e.g. **9**, Figure 1).[30] Those glycomimetics are, however, not effective in fibroblast of GD patients hosting domain II-located mutations. To the best of our knowledge, the only documented example of a chaperone effect in the L444P/P415R GCase variant reports a 1.5-fold activity enhancement using 4-[(2-amino-3,5-dibromophenyl)methylamino]cyclohexan-1-ol (ambroxol; **7**, Figure 1) at a concentration of 50 μM.[67] In the present study, the βCD formulation with compound **21**, bearing the shortest aglycone substituent, displayed the highest chaperone effect in V230G/R296X GD fibroblasts among the series (2.7-fold GCase activity enhancement at 20 μM). Compound **22**, differing only in a tetrafluoromethylene segment, also promoted a significant GCase activity enhancement (1.8-fold at 20 μM), whereas the homologs **23** and **24**, in which the hydrocarbon moiety increases

from four to nine methylene groups, were inactive. Remarkably, the very severe GD L444P/P415R mutation responded to the four fluorinated sp^2-iminosugar (**21**-**24**):βCD complexes, with a 1.7- to 1.9-fold increased activity for **21**, **23** and **24** and of up to 2.9-fold in the case of the **22**:βCD formulation at 20 μM.

The adult neuronopathic type 3 GD-associated N188S/G183W mutation is located in the catalytic domain (domain III) and has previously been found to be reactive to sp^2-iminosugars with distortable cores such as **9** or **10** (Figure 1).[30,32] In stark contrast, the homozygous L444P variant, having the highest prevalence among neuronopathic GD patients, has been found to respond only to undistortable sp^2-iminosugars such as **22** (Figure 1), with mutant GCase activity enhancements being 1.6-fold at a chaperone concentration of 2-25 μM.[39] A similar result was obtained with the new fluorinated sp^2-iminosugars **21** and **24** in complex with βCD when administered at 20 μM. The **22**:βCD formulation performed outstandingly better in this variant, reaching an unprecedented 2-fold mutant enzyme activity enhancement at a concentration of only 2 μM and increasing to 2.8-fold at 20 μM.

The results above discussed highlight the potential of the strategy based on the use of 1,6-anhydro-L-idonojirimycin undistortable glycomimetics with fluorinated aglycones, in complex with β-cyclodextrin, to develop a chaperone therapy against the neuronopathic forms of Gaucher disease, including highly challenging domain II-located GCase mutations. However, note that the widely investigated piperidine-type GCase inhibitor *N*-nonyl-1-deoxynijirimycin (NN-DNJ; **1**, Figure 1), which is able to enhance N370S GCase activity by 65% and is frequently used as a reference pharmacological chaperone for GD, did not show any activity in the L444P GCase mutant in our work not in that of others.[32,68] In order to confirm that the mechanism of action involves rescuing and trafficking restoration of the endogenous mutant GCase, immunolabeling

and colocalization experiments were further conducted using fibroblasts from type 2 GD patients bearing the L444P/P415R mutation (Figure 5). The left panel shows a series of confocal fluorescence microscopy images after immunostaining of the ER (protein disulfide isomerase, PDI; red), GCase (green) and the nucleus (Hoechst; blue), as well as the corresponding merged images, in healthy control fibroblasts and in L444P/P415R GD fibroblasts before and after treatment with **22**:βCD at 20 μM. It can be observed that the GCase content in the cells of GD patients is much lower than in the control and that it colocalizes with the ER (yellow spots), in agreement with impaired traffic to the lysosome. After treatment with the chaperone:βCD complex, the amount of GCse increases very significantly and it is no longer located in the ER. The right panel, in which the lysosome (lysosome associated membrane protein 2, LAMP-2; red), instead of the ER, has been labeled, shows that after treatment with the chaperone, GCase colocalizes with this organelle as it happens in the control cells. Although full validation will require *in situ* GCase activity measurements,[69,70] this result complements the *in vitro* assays and strongly supports that the observed enzyme activity enhancements correspond indeed to the lysosomal and not to the cytoplasmatic GCase component.[32,33]

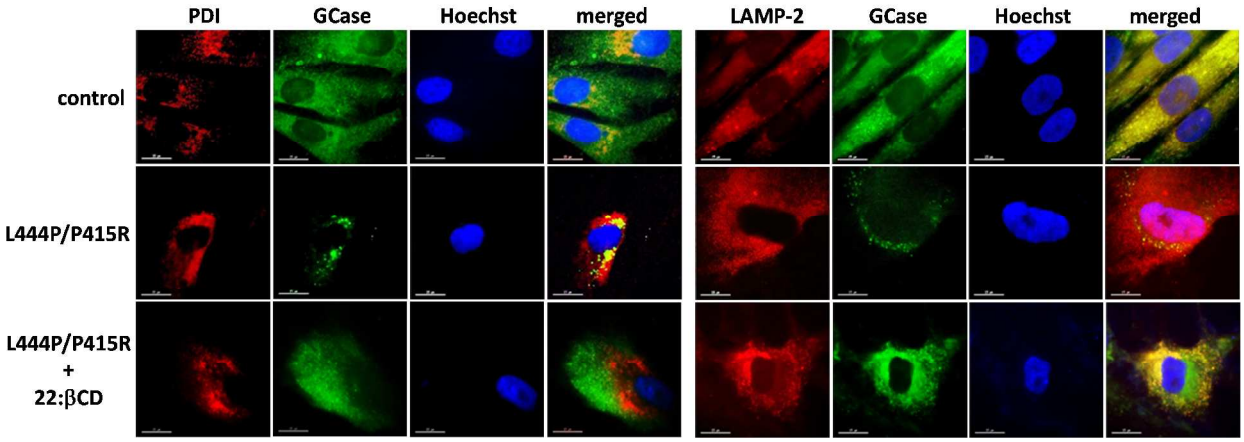

Figure 5. Effect of **22**:βCD on the traffic of GCase from the ER to lysosomes in L444P/P415R type 2 Gaucher fibroblasts. Fibroblasts were treated with 20 μM of the complexed chaperone.

Left panel: ER marker (protein disulfide isomerase, PDI) or GCase are visualized as red or green, respectively; in the merged images, yellow denotes colocalization in the ER. Right panel: lysosomal marker (lysosome associated membrane protein 2, LAMP-2) or GCase are visualized as red or green, respectively; in the merged images, yellow denotes colocalization in lysosomes. Scale bar = 15 μm. The shown pictures are representative of more than 100 cells in 10 randomly obtained images.

Chaperone-GCase Docking Experiments. Although the responsiveness of mutant GCase to chaperone therapy is clearly patient-dependent, the set of the results indicates that the fluorinated sp^2-iminosugar **22** has a remarkably broader activity profile when compared to the other compounds in the series, being able to promote very significant enzyme activity enhancements in GCase variants bearing mutations in any of the three protein domains, including the highly refractory domain II-located L444P/P415R and L444P/L444P mutants. In order to obtain structural information on the interactions operating in chaperone:GCase complex stabilization, binding of **22** to GCase was studied next by means of docking and MD simulations. The bicyclic core binds to the active site, with the hydroxyl groups involved in a hydrogen-bonding network with the surrounding amino acids (Asn127, Asn234, Arg395). Contrary to the observations for other amphiphilic GCase ligands, the N-substituent does not locate above the hydrophobic channel at the entrance of the active site, but turns instead to the catalytic site area establishing a number of fluor-aromatic contacts (Figure 6). The resulting very compact arrangement was stable along the 20 ns MD trajectory computed. This is in agreement with the observed strong influence of structural modifications in the hydrocarbon or perfluorocarbon segments related to the chaperoning capabilities of the PC, probably being responsible for the unprecedented broad mutation-range GCase rescuing capabilities of **22**.

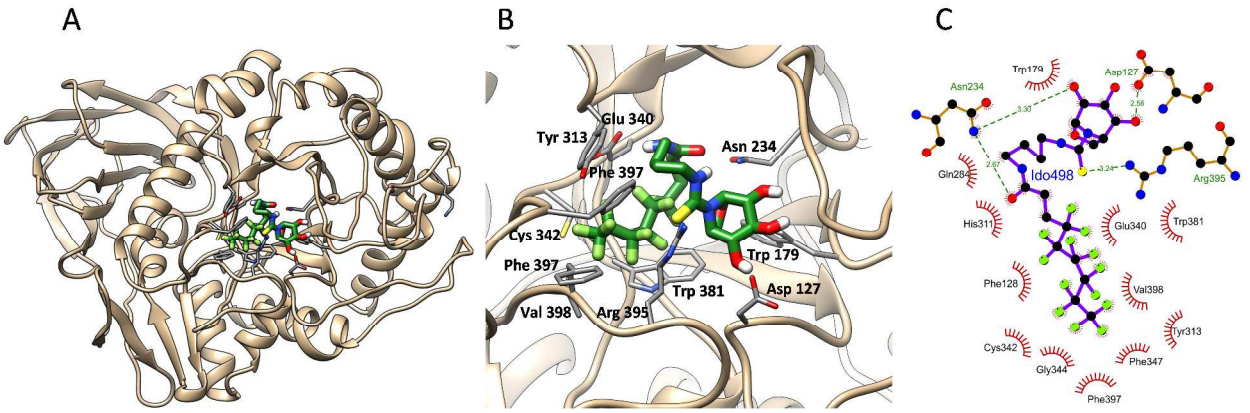

Figure 6. Docking of **22** to the human β-glucocerebrosidase structure (see Experimental Section for details). A) View of the enzyme surface showing the active site; the docked molecule is represented by sticks. B) Detail of the active site cavity, with the docked molecule inside (carbon in green, fluor in light green, nitrogen in blue, oxygen in red, sulfur in yellow, hydrogen in white; hydrogen atoms linked to carbon are omitted for clarity). Amino acid residues in closest contact with the chaperone are also depicted. C) Diagram showing the interactions between the protein and the ligand. Images correspond to the MD snapshot closest to the average structure.

Conclusions

The set of results discussed herein provides solid proof of the concept concerning the suitability of the sp^2-iminosugar prototype based on AIJ undistortable glycomimetics with fluorinated substituents, fitting in the GCase active site, for the development of PC candidates targeting the neuronopathic forms of Gaucher disease. Formulation of the fluorinated PC with β-cyclodextrin prevents unwanted side effects arising from aggregation while warranting the efficient transfer of the drug to the enzyme in the ER, thereby bypassing the UPR and restoring trafficking to the lysosome, as confirmed by immunolabeling and colocalization studies. Docking experiments underlined the importance of fine-tuning the flexibility of the molecule to

optimize the contacts between the fluorinated portion and the protein in order to achieve high activity enhancements for a broad range of GD causative single nucleotide GCase polymorphs. Since other lysosomal glycosidases also have lipophilic pockets with aromatic amino acids in the vicinity of the catalytic site,[19] the incorporation of fluorinated moieties onto glycomimetic scaffolds showing stereocomplementarity with the putative sugar substrates can be generalized for the design of PCs targeting a range of LSDs. Interestingly, UPR-inducing mutations in GCase, even when asymptomatic for GD, represent the strongest risk factor for developing Parkinson disease (PD) hitherto identified.[71,72] Indeed, the possibility of using PCs for neuroprotection therapy in PD has already been confirmed in mutant mice and in PD fibroblasts[73] and neurons,[74] further highlighting the importance of developing efficient strategies for PC optimization. Further studies on the potential of fluorinated sp^2-iminosugars in formulation with cyclodextrins to tackle both LSDs and PD are currently being carried out in our laboratories.

Experimental Section

General Methods. Reagents and solvents were purchased from commercial sources and used without further purification. Optical rotations were measured with a JASCO P-2000 polarimeter, using a sodium lamp (λ = 589 nm) at 22 ºC in 1 cm or 1 dm tubes. IR spectra were recorded on a JASCO FTIR-410 device. UV spectra were recorded on JASCO V-630 instrument; unit for ε values: $mM^{-1}cm^{-1}$. NMR experiments were performed at 300 (75.5), 400 (100.6) and 500 (125.7) MHz. 1-D TOCSY as well as 2-D COSY and HMQC experiments were carried out to assist signal assignment. In the FABMS spectra, the primary beam consisted of Xe atoms with a maximun energy of 8 keV. The samples were dissolved in *m*-nitrobenzyl alcohol or thioglycerol

as the matrices and the positive ions were separated and accelerated above a potencial of 7 keV. NaI was added as cationizing agent. For ESI mass spectra, 0.1 pM sample concentrations were used, the mobile phase consisting of 50% aq MeCN at 0.1 mL min^{-1}. Thin-layer chromatography was performed on precoated TLC plates, silica gel 30F-245, with visualization by UV light and also with 10% H_2SO_4 or 0.2% w/v cerium (IV) suphate-5% ammonium molybdate in 2 M H_2SO_4 or 0.1% ninhydrin in EtOH. Column chromatography was performed on Chromagel (silice 60 AC.C 70-200 μm). All compounds were purified to ≥95% purity as determined by elemental microanalysis results obtained on a CHNS-TruSpect® Micro elemental analyzer (Instituto de Investigaciones Químicas de Sevilla, Spain) from vacuum-dried samples. The analytical results for C, H, N and S were within ±0.5 of the theoretical values.

Materials. 4-(*tert*-Butoxycarbonylamino)butyl isothiocyanate, 4,4,5,5,6,6,7,7,7-nonafluoroheptanoic acid, and 4,4,5,5,6,6,7,7,8,8,9,9,9-tridecafluorononanoic acid were purchased from commercial sources. *N*-(*tert*-Butoxycarbonyl)nonanediamine[75] and 5-amino-5-deoxy-1,2-*O*-isopropylidene-β-L-idofuranose[59] (**12**) were synthesized using the previously described routes.

9-(*tert*-Butoxycarbonylamino)nonyl Isothiocyanate (14). $CSCl_2$ (0.87 mL, 11.4 mmol) was added to a heterogeneous mixture of *N*-(*tert*-butoxycarbonyl)nonanediamine[75] (737 mg, 2.85 mmol) in 1:1 DMC-H_2O (32 mL) and $CaCO_3$ (2.3 g, 23 mmol), $CSCl_2$ (0.87 mL, 11.4 mmol) was added at 0 ºC. The reaction mixture was vigorously stirred for 2 h at rt and the organic phase was separated. The aqueous phase was extracted with DCM (3 x 15 mL), the combined extracts were dried ($MgSO_4$), concentrated, and the resulting residue was purified by column chromatography (1:8→1:4 EtOAc-petroleum ether). Yield: 599 mg (56%). R_f 0.50 (1:4 EtOAc-petroleum ether). IR (ATR) ν_{max} 2177 cm^{-1}. ^1H NMR (300 MHz, $CDCl_3$) δ 4.50 (bs, 1 H, NH),

3.50 (t, 2 H, $^3J_{H,H}$ = 6.6 Hz, CH_2NCS), 3.09 (m, 2 H, CH_2NHCO), 1.68 (m, 2 H, CH_2), 1.45 (s, 9 H, CMe_3), 1.39 (m, 12 H, CH_2). ^{13}C NMR (125.7 MHz, $CDCl_3$) δ 156.0 (CO), 129.9 (NCS), 79.0 (*C*Me_3), 45.0 (*C*H_2NCS), 40.6 (*C*H_2NHCO), 30.0 29.9, 29.3, 29.1, 28.7 (CH_2), 28.4 (C*Me*$_3$), 26.7, 26.5 (CH_2). ESIMS: *m/z* 323 $[M + Na]^+$. Anal. Calcd for $C_{15}H_{28}N_2O_2S$: C, 59.96; H, 9.39; N, 9.32; S, 10.67. Found: C, 60.09; H, 9.43; N, 9.24; S, 10.48.

5-[*N*'-(4-*tert*-Butoxycarbonylaminobutyl)thioureido]-5-deoxy-1,2-*O*-isopropylidene-β-L-idofuranose (15). Et_3N (0.6 mL, 4.3 mmol) and isothiocyanate **13** (0.94 mmol, 1.1 eq) were added to a solution of 5-amino-5-deoxy-1,2-*O*-isopropylidene-β-L-idofuranose[59] (**12**, 188 mg, 0.86 mmol) in pyridine (5 mL). The mixture was stirred at rt for 18 h and concentrated. The resulting residue was coevaporated several times with toluene and purified by column chromatography using 50:1 → 40:1 DCM-MeOH as the eluent. Yield: 317 mg (82%; colorless syrup). $[\alpha]_D$ −68.4 (*c* 1.0 in DCM). R_f 0.22 (100:10:1 DCM-MeOH-H_2O). UV (DCM) 242 nm (ε_{mM} 14.1). ^{1}H NMR (500 MHz, CD_3OD, 323 K) δ 5.98 (d, 1 H, $J_{1,2}$ = 3.7 Hz, H-1), 4.66 (m, 1 H, H-5), 4.58 (d, 1 H, H-2), 4.39 (dd, 1 H, $J_{4,5}$ = 7.8 Hz, $J_{3,4}$ = 2.6 Hz, H-4), 4.22 (d, 1 H, H-3), 3.83 (dd, 1 H, $J_{6a,6b}$ = 11.2 Hz, $J_{5,6a}$ = 4.3 Hz, H-6a), 3.80 (dd, 1 H, $J_{5,6b}$ = 4.8 Hz, H-6b), 3.57 (m, 2 H, CH_2NHCS), 3.15 (m, 2 H, $^3J_{H,H}$ = 6.7 Hz, CH_2NHBoc), 1.68 (m, 2 H, CH_2), 1.60 (m, 2 H, CH_2), 1.54, 1.38 (2 s, 6 H, CMe_2), 1.52 (s, 9 H, CMe_3), 1.37 (m, 4 H, CH_2). ^{13}C NMR (125.7 MHz, CD_3OD, 323 K) δ 183.7 (CS), 158.5 (CO), 112.8 (*C*Me_2), 105.8 (C-1), 87.0 (C-2), 81.2 (C-4), 80.0 (*C*Me_3), 75.8 (C-3), 62.7 (C-6), 56.2 (C-5), 45.1 (*C*H_2NHCS), 41.1 (*C*H_2NHBoc), 28.8 (C*Me*$_3$), 28.3, 27.5 (CH_2), 27.0, 264 (C*Me*$_2$). ESIMS: *m/z* 472 $[M + Na]^+$. Anal. Calcd for $C_{19}H_{35}N_3O_7S$: C, 50.76; H, 7.85; N, 9.35; S, 7.13. Found: C, 50.74; H, 7.60; N, 9.57; S, 6.97.

5-[*N*'-(9-*tert*-Butoxycarbonylaminononyl)thioureido]-5-deoxy-1,2-*O*-isopropylidene-β-L-idofuranose (16). Et_3N (0.6 mL, 4.3 mmol) and isothiocyanate **14** (0.94 mmol, 1.1 eq) were

added to a solution of 5-amino-5-deoxy-1,2-*O*-isopropylidene-β-L-idofuranose[59] (**12**, 188 mg, 0.86 mmol) in pyridine (5 mL). The mixture was stirred at rt for 18 h and concentrated. The resulting residue was coevaporated several times with toluene and purified by column chromatography using 30:1→15:1 CH_2Cl_2-MeOH as the eluent. Yield: 286 mg (64%; white amorphous solid). $[\alpha]_D$ −58.8 (*c* 1.0 in DCM). R_f 0.40 (15:1 DCM-MeOH). UV (DCM) 248 nm (ε_{mM} 14.1). ^{1}H NMR (500 MHz, $CDCl_3$, 313 K) δ 6.65 (bs, 1 H, NH), 5.99 (d, 1 H, $J_{1,2}$ = 3.7 Hz, H-1), 4.84 (bs, 1 H, H-5), 4.60 (bs, 1 H, NH), 4.54 (d, 1 H, H-2), 4.32 (d, 1 H, $J_{3,4}$ = 2.1 Hz, H-3), 4.29 (m, 1 H, H-4), 4.22 (bs, 1 H, NH), 3.92 (dd, 1 H, $J_{6a,6b}$ = 11.2 Hz, $J_{5,6a}$ = 4.6 Hz, H-6a), 3.76 (dd, 1 H, $J_{5,6b}$ = 5.4 Hz, H-6b), 3.41 (bs, 2 H, C*H*$_2$NHCS), 3.30 (bs, 1 H, OH), 3.11 (m, 2 H, C*H*$_2$NHBoc), 19.1 (bs, 1 H, OH), 1.58 (m, 2 H, C*H*$_2$CH$_2$NHCS), 1.52, 1.33 (2 s, 6 H, CMe_2), 1.50 (m, 2 H, CH_2), 1.46 (s, 9 H, CMe_3), 1.32 (m, 10 H, CH_2). ^{13}C NMR (125.7 MHz, $CDCl_3$, 313 K) δ 182.1 (CS), 156.2 (CO), 111.9 (*C*Me$_2$), 104.6 (C-1), 85.0 (C-2), 80.5 (C-4), 79.2 (*C*Me$_3$), 75.4 (C-3), 63.9 (C-6), 54.9 (C-5), 44.7 (*C*H$_2$NHCS), 40.6 (*C*H$_2$NHBoc), 29.9, 29.2, 28.9, 28.8, 28.7 (CH_2), 28.5 (CH_2, C*Me*$_3$), 26.8, 26.1 (C*Me*$_2$), 26.7 (CH_2). ESIMS: *m/z* 542 [M + Na]$^+$. Anal. Calcd for $C_{24}H_{45}N_3O_7S$: C, 55.47; H, 8.73; N, 8.09; S, 6.17. Found: C, 55.41; H, 8.71; N, 8.08; S, 6.03.

***N*-[*N*'-(4-Aminobutyl)thiocarbamoyl]-1,6-anhydro-α-L-idonojirimycin Hydrochloride (17).** A solution of **15** (0.52 mmol) in 90% TFA-H_2O (3 mL) was stirred at rt for 30 min, concentrated under reduced pressure, coevaporated several times with water, neutralized with Amberlite IRA-68 (OH^-) ion-exchange resin, and subjected to column chromatography using 6:1:1→6:2:1 CH_3CN-H_2O-NH_4OH as the eluent. The product thus obtained was dissolved in water, HCl 0.1 M was added to until pH 5.0, and the resulting solution was freeze-dried. Yield: 141 mg (93%; white foam). $[\alpha]_D$ +41.5 (*c* 1.0 in MeOH). R_f 0.25 (6:3:1 CH_3CN-H_2O-NH_4OH).

UV (H_2O) 242 nm (ε_{mM} 16.2). ^{1}H NMR (500 MHz, D_2O, 323 K) δ 6.13 (s, 1 H, H-1), 5.05 (m, 1 H, H-5), 4.34 (d, 1 H, $J_{6a,6b}$ = 8.5 Hz, H-6a), 4.05 (dd, 1 H, $J_{5,6b}$ = 5.0 Hz, H-6b), 3.94 (m, 1 H, H-4), 3.81 (m, 4 H, H-2, H-3, CH_2NHCS), 3.00 (t, 2 H, $J_{H,H}$ = 7.3 Hz, CH_2NH$_2$), 1.85 (m, 2 H, CH_2), 1.77 (m, 2 H, CH_2). ^{13}C NMR (125.7 MHz, D_2O, 323 K) δ 178.0 (CS), 88.8 (C-1), 75.7 (C-3), 74.0 (C-2), 71.0 (C-4), 66.6 (C-6), 58.9 (C-5), 45.5 (*C*H_2NHCS), 40.5 (CH_2NH_2), 27.5, 26.7 (CH_2). ESIMS: *m/z* 292 $[M + H]^+$. Anal. Calcd for $C_{11}H_{22}ClN_3O_4S$: C, 40.30; H, 6.76; N, 12.82; S, 9.78. Found: C, 40.65; H, 6.47; N, 12.58; S, 9.55.

***N*-[*N*'-(9-Aminononyl)thiocarbamoyl]-1,6-anhydro-α-L-idonojirimycin Hydrochloride (18).** A solution of **16** (0.52 mmol) in 90% TFA-H_2O (3 mL) was stirred at rt for 30 min, concentrated under reduced pressure, coevaporated several times with water, neutralized with Amberlite IRA-68 (OH^-) ion-exchange resin, and subjected to column chromatography using 10:1 CH_3CN-H_2O as the eluent. The product thus obtained was dissolved in water, HCl 0.1 M was added to until pH 5.0, and the resulting solution was freeze-dried. Yield: 160 mg (85%; white foam). $[\alpha]_D$ +41.6 (*c* 1.0 in MeOH). R_f 0.27 (10:1:1 CH_3CN-H_2O-NH_4OH). UV (MeOH) 249 nm (ε_{mM} 14.6). ^{1}H NMR (500 MHz, D_2O, 313 K) δ 6.05 (s, 1 H, H-5), 4.96 (dd, 1 H, $J_{1,7b}$ = 5.0 Hz, $J_{1,2}$ = 4.1 Hz, H-1), 4.25 (d, 1 H, $J_{7a,7b}$ = 8.5 Hz, H-6a), 3.96 (dd, 1 H, H-6b), 3.85 (dd, 1 H, $J_{2,3}$ = 8.4 Hz, H-2), 3.73 (m, 2 H, H-4, H-3), 3.69 (td, 2 H, $J_{H,H}$ = 7.1 Hz, $J_{CH,NH}$ = 3.4 Hz, CH_2NHCS), 3.09 (t, 2 H, $J_{H,H}$ = 7.5 Hz, CH_2NH$_2$), 1.73 (m, 4 H, CH_2), 1.45 (m, 14 H, CH_2). ^{13}C NMR (125.7 MHz, D_2O, 313 K) δ 177.5 (CS), 88.5 (C-5), 75.2 (C-3), 74.07 (C-4), 70.8 (C-2), 66.2 (C-7), 58.4 (C-1), 45.6 (*C*H_2NHCS), 39.8 (CH_2NH_2), 28.5, 28.4, 28.2, 26.8, 26.0, 25.7 (CH_2). FABMS: *m/z* 384 (90, $[M + Na]^+$), 362 (20, $[M + H]^+$). HRFABMS Calcd for $C_{16}H_{31}N_3O_4S$ $[M + Na]^+$ 384.1933, found 384.1925.

***N*-[*N*'-[4-(4,4,5,5,6,6,7,7,7-Nonafluoroheptanamido)butyl]thiocarbamoyl]-1,6-anhydro-α-L-idonojirimycin (21).** TBTU (79 mg, 0.25 mmol) and DIEA (162 μL, 0.95 mmol) were added to a solution of the amine **17** (0.25 mmol) and the carboxylic acid **19** (0.19 mmol) in DMF (10 mL), under Ar atmosphere. The reaction mixture was stirred at rt for 18 h and the solvent was removed under reduced pressure. The resulting residue was purified by column chromatography using 100:10:0.5→70:10:0.5→50:10:0.5 DCM-MeOH-NH_4OH as the eluent. Yield: 75 mg (70%; white amorphous solid). $[\alpha]_D$ +24.3 (*c* 1.0 in MeOH). R_f 0.44 (45:5:3 EtOAc-EtOH-H_2O). UV (MeOH) 249 nm (ε_{mM} 7.9). ^{1}H NMR (500 MHz, CD_3OD) δ 5.82 (bs, 1 H, H-1), 4.88 (m, 1 H, H-5), 4.09 (d, 1 H, $J_{6a,6b}$ = 7.8 Hz, H-6a), 3.75 (dd, 1 H, $J_{5,6b}$ = 5.1 Hz, H-6b), 3.63 (m, 3 H, H-4, C*H*$_2$NHCS), 3.54 (m, 2 H, H-2, H-3), 3.23 (m, 2 H, C*H*$_2$NHCO), 2.52 (m, 4 H, CH_2CO, CH_2CF_2), 1.66 (m, 2 H, CH_2), 1.55 (m, 2 H, CH_2). ^{13}C NMR (125.7 MHz, CD_3OD) δ 180.8 (CS), 172.8 (CO), 90.2 (C-1), 77.4 (C-3), 75.8 (C-2), 72.4 (C-4), 66.8 (C-6), 60.0 (C-5), 45.9 (*C*H_2NHCS), 40.3 (*C*H_2NHCO), 27.8, 27.6, 27.3 (CH_2). ESIMS: *m/z* 565.5 $[M + Na]^+$. Anal. Calcd for $C_{18}H_{24}F_9N_3O_5S$: C, 38.23; H, 4.28; N, 7.43; S, 5.67. Found: C, 38.09; H, 4.53; N, 7.19; S, 5.31.

***N*-[*N*'-[4-(4,4,5,5,6,6,7,7,8,8,9,9,9-Tridecafluorononanamido)butyl]thiocarbamoyl]-1,6-anhydro-α-L-idonojirimycin (22).** Compound **22** was obtained from amine **17** (0.25 mmol) and carboxylic acid **20** (0.19 mmol) following the procedure described above for **21**. Column chromatography, eluent 100:10:0.5 →70:10:0.5→40:10:0.5 DCM-MeOH-NH_4OH. Yield: 97 mg (77%; white amorphous solid). $[\alpha]_D$ +33.4 (*c* 1.0 in MeOH). R_f 0.39 (45:5:3 EtOAc-EtOH-H_2O). UV (MeOH) 248 nm (ε_{mM} 9.0). ^{1}H NMR (400 MHz, CD_3OD) δ 5.84 (bs, 1 H, H-1), 4.88 (m, 1 H, H-5), 4.12 (d, 1 H, $J_{6a,6b}$ = 7.9 Hz, H-6a), 3.77 (dd, 1 H, $J_{5,6b}$ = 5.1 Hz, H-6b), 3.65 (m, 3 H, H-4, C*H*$_2$NHCS), 3.57 (m, 2 H, H-2, H-3), 3.25 (t, 2 H, $J_{H,H}$ = 7.0 Hz, C*H*$_2$NHCO), 2.54 (m, 4 H,

CH_2CO, CH_2CF_2), 1.68 (m, 2 H, CH_2), 1.58 (m, 2 H, CH_2). ^{13}C NMR (100.6 MHz, CD_3OD) δ 180.8 (CS), 172.7 (CO), 90.2 (C-1), 77.3 (C-3), 75.8 (C-2), 72.4 (C-4), 66.8 (C-6), 60.0 (C-5), 45.9 (*C*H_2NHCS), 40.3 (*C*H_2NHCO), 27.8, 27.6, 27.3 (CH_2). ESIMS: *m/z* 664.2 $[M - H]^-$. Anal. Calcd for $C_{20}H_{24}F_{13}N_3O_5S$: C, 36.10; H, 3.64; N, 6.31; S, 4.82. Found: C, 35.87; H, 3.93; N, 6.33; S, 4.58.

***N*-[*N*'-[4-(4,4,5,5,6,6,7,7,7-Nonafluoroheptanamido)nonyl]thiocarbamoyl]-1,6-anhydro-α-L-idonojirimycin (23).** Compound **23** was obtained from amine **18** (0.25 mmol) and carboxylic acid **19** (0.19 mmol) following the procedure described above for **21**. Column chromatography, eluent 100:10:0.5→70:10:0.5→40:10:0.5 DCM-MeOH-NH_4OH. Yield: 87 mg (72%; white amorphous solid). $[\alpha]_D$ +27.7 (*c* 1.0 in MeOH). R_f 0.64 (45:5:3 EtOAc-EtOH-H_2O). UV (MeOH) 248 nm (ε_{mM} 9.8). ^1H NMR (500 MHz, CD_3OD) δ 5.85 (bs, 1 H, H-1), 4.90 (m, 1 H, H-5), 4.12 (d, 1 H, $J_{6a,6b}$ = 7.9 Hz, H-6a), 3.77 (dd, 1 H, $J_{5,6b}$ = 5.1 Hz, H-6b), 3.70 (m, 1 H, H-4), 3.61 (m, 2 H, C*H*$_2$NHCS) 3.58 (m, 2 H, H-2, H-3), 3.21 (t, 2 H, $J_{H,H}$ = 7.1 Hz, C*H*$_2$NHCO), 2.54 (m, 4 H, CH_2CO, CH_2CF_2), 1.65 (m, 2 H, CH_2), 1.53 (m, 2 H, CH_2), 1.37 (m, 10 H, CH_2). ^{13}C NMR (125.7 MHz, CD_3OD) δ 180.8 (CS), 172.6 (CO), 90.2 (C-1), 77.4 (C-3), 75.8 (C-2), 72.5 (C-4), 66.8 (C-6), 60.1 (C-5), 46.5 (*C*H_2NHCS), 40.6 (*C*H_2NHCO), 30.5, 30.3, 30.3, 29.9, 27.9, 27.8, 27.7 (CH_2). ESIMS: *m/z* 658.4 $[M + Na]^+$. Anal. Calcd for $C_{23}H_{34}F_9N_3O_5S$: C, 43.46; H, 5.39; N, 6.61; S, 5.04. Found: C, 43.37; H, 5.66; N, 6.49; S, 4.89.

***N*-[*N*'-[4-(4,4,5,5,6,6,7,7,8,8,9,9,9-Tridecafluorononanamido)nonyl]thiocarbamoyl]-1,6-anhydro-α-L-idonojirimycin (24).** Compound **24** was obtained from amine **18** (0.25 mmol) and carboxylic acid **20** (0.19 mmol) following the procedure described above for **21**. Column chromatography, eluent 100:10:0.5→70:10:0.5→40:10:0.5 DCM-MeOH-NH_4OH. Yield: 119 mg (85%; white amorphous solid). $[\alpha]_D$ +22.8 (*c* 1.0 in MeOH). R_f 0.63 (45:5:3 EtOAc-EtOH-

H_2O). UV (MeOH) 249 nm (ε_{mM} 13.1). ^{1}H NMR (500 MHz, CD_3OD) δ 5.85 (bs, 1 H, H-1), 4.90 (m, 1 H, H-5), 4.12 (d, 1 H, $J_{6a,6b}$ = 7.9 Hz, H-6a), 3.77 (dd, 1 H, $J_{5,6b}$ = 5.2 Hz, H-6b), 3.68 (m, 1 H, H-4), 3.61 (m, 2 H, C*H*$_2$NHCS), 3.58 (m, 2 H, H-2, H-3), 3.21 (t, 2 H, $J_{H,H}$ = 7.1 Hz, C*H*$_2$NHCO), 2.54 (m, 4 H, CH_2CO, CH_2CF_2), 1.65 (m, 2 H, CH_2), 1.54 (m, 2 H, CH_2), 1.37 (m, 10 H, CH_2). ^{13}C NMR (125.7 MHz, CD_3OD) δ 180.9 (CS), 172.7 (CO), 90.2 (C-1), 77.4 (C-3), 75.9 (C-2), 72.5 (C-4), 66.8 (C-6), 60.1 (C-5), 46.5 (*C*H_2NHCS), 40.6 (*C*H_2NHCO), 30.6, 30.4, 30.3, 30.0, 28.1, 28.0, 27.9, 27.7, 27.6 (CH_2). ESIMS: *m/z* 758.4 $[M + Na]^+$. Anal. Calcd for $C_{25}H_{34}F_{13}N_3O_5S$: C, 40.82; H, 4.66; N, 5.71; S, 4.36. Found: C, 40.86; H, 4.52; N, 5.54; S, 4.07.

Commercial Enzyme Inhibition Assays. Inhibition constant (K_i) values were determined by spectrophotometrically measuring the residual hydrolytic activities of the glycosidases against the respective *o*- (for β-galactosidase from *E. coli*) or *p*-nitrophenyl α- or β-D-glycopyranoside (for other glycosidases) in the presence of the iminosugars. Each assay was performed in phosphate buffer or phosphate-citrate buffer (for α- or β-mannosidase and amyloglucosidase) at the optimal pH for the enzymes. The reactions were initiated by addition of the enzyme to a solution of the substrate in the absence or presence of various inhibitor concentrations. The mixture was incubated for 10-30 min at 37 ºC or 55 ºC (for amyloglucosidase) and the reaction was quenched by addition of 1 M Na_2CO_3. Reaction times were appropriate to obtain 10-20% conversion of the substrate in order to achieve linear rates. The absorbance of the resulting mixture was determined at 405 nm. Approximate values of K_i were determined using a fixed concentration of substrate (around the K_M value for the different glycosidases) and various inhibitor concentrations. Full K_i determinations and the enzyme inhibition mode were determined from the slope of Lineweaver-Burk plots and double reciprocal analysis. Representative examples of the Lineweaver-Burk plots are shown in Figures S11-S18.

Critical Micellar Concentration (CMC) Determinations. CMC was determined using a methodology based on the environmental dependence of pyrene fluorescence.[60] A pyrene stock solution (1 mM in THF) was diluted with Milli-Q water to give a final concentration of 0.6 μM. This solution was subsequently used to prepare solutions of iminosugars ranging from 1180 to $4.3 \cdot 10^{-3}$ μM. The samples were allowed to equilibrate for 1 h at 37 °C. Measurements were carried out at λ_{em} 375 nm. The ratio of the fluorescence intensities at λ_{ex} 339 (I_{339}) and 335 (I_{335}) nm was used to quantify the shift of the broad excitation band. Finally, the critical aggregation concentrations were determined from the crossover point when representing the log[iminosugar] *vs* I_{339}/I_{335} ratio (See SI, Figures S19-S22).

NMR-Monitoring of Chaperone:βCD Complex Formation, Titration Experiments and Association Constant Determinations. ^{1}H NMR spectra of 1 mM suspensions or solutions of the fluorinated sp^2-iminosugars **21**-**24** (5% DMSO-d_6 in D_2O) were registered at 298 K in the absence and in the presence of equimolecular amounts of βCD. The rise of the intensity of the sp^2-iminosugar resonances upon addition of βCD was indicative of the solubilizing capabilities of βCD. On the other hand, the up-field shifts of ^{1}H NMR βCD signals (especially H-3 and H-5 resonances) unequivocally demontrated the formation of an inclusion complex (Figures S24-S27). Association constants (K_{as}) for the complexes **21**:βCD and **22**:βCD were additionally determined in D_2O at 298 K by measuring the chemical shift variations either in the ^{1}H or ^{19}F NMR spectra (500 and 376 MHz, respectively) of a solution of one of the components in the presence of increasing amounts of its counterpart. In a typical titration experiment, a stock solution of βCD (0.3-0.5 mM) in D_2O was prepared. A 500 μL-aliquot of this solution was transferred to a NMR tube and the initial NMR spectrum was recorded. Then, a solution (2-4 mM) of the chaperone was prepared in the stock βCD solution in order to maintain the host

concentration constant all throughout the titration experiment. Aliquots of the iminosugar solution were sequentially added to the NMR tube and the corresponding spectrum was recorded after each addition until 90-100% complexation had been achieved. The chemical shifts of the βCD signals obtained at ca. 12-15 different host-guest concentration ratios were plotted against the iminosugar concentration and used in an iterative least-squares fitting procedure.[62,76] Alternatively, the titration experiment was reproduced inversely, by adding to a stock solution of the iminosugar (ca. 0.5 mM) increasing amounts of a concentrated solution of βCD and monitoring the ^{19}F NMR resonance shifts of the fluorocarbonated chain upon complexation. Both, the direct and inverse K_a determination procedures afforded qualitatively similar results (See SI, Figures S28-S32).

Measurement of Purified Human GCase Inhibition Activities *in vitro*. GCase activities were determined as above using purified human GCase, obtained from Genzyme (Genzyme Japan, Tokyo, Japan) in 0.1 M citrate buffer at pH 5 or pH 7 and 4-methylumbelliferone (4-MU)-conjugated β-D-glucopyranoside as the substrate. The reactions were terminated by adding 0.2 mL of 0.2 M glycine sodium hydroxide buffer (pH 10.7). The liberated 4-methylumbelliferone was measured in a black-well plate with a Perkin Elmer Luminescence Spectrometer (excitation wavelength: 340 nm; emission: 460 nm).

Profiling of the Inhibitory Selectivity Towards Lysosomal Glycosidases by *in vitro* Enzyme Assay. For determination of lysosomal enzyme activities in cell lysates, cells were scraped into ice-cold H_2O (10^6 cells mL^{-1}) and lysed by sonication. Insoluble materials were removed by centrifugation at 15,000 rpm for 5 min and protein concentrations were determined with Protein Assay Rapid Kit (WAKO, Tokyo, Japan). 10 μL of the lysates in 0.1% Triton X-100 in distilled water were incubated at 37 °C with 20 μL of the substrate solution in 0.1 M

citrate buffer, pH 4.5, in absence or presence of increasing concentrations of the chaperones or their complexes with βCD. The substrates were 4-methylumbelliferone (4-MU)-conjugated β-D-glucopyranoside (for GCase), α-D-glucopyranoside (for α-glucosidase), α-D-galactopyranoside (for α-Galase), β-D-galactopyranoside (for β-galactosidase), *N*-acetyl-β-D-glucosaminide (for total β-hexosaminidase) and α-*N*-acetyl-D-galactosaminide for α-*N*-acetylgalactosaminidase. GCase activities in cell lysates were also determined in 0.1 M citrate buffer at pH 5 or pH 7, supplemented with sodium taurocholate (0.8% w/v). The reactions were terminated by adding 0.2 mL of 0.2 M glycine sodium hydroxide buffer (pH 10.7). The liberated 4-methylumbelliferone was measured in the black-well plate with a Perkin Elmer Luminescence Spectrometer (excitation wavelength: 340 nm; emission: 460 nm). One unit of enzyme activity was defined as nmol of 4-methylumbelliferone released per hour and normalized for the amount of protein contained in the lysates. The fluorinated chaperones **21**-**24**, either in free form or complexed with βCD, showed total selectivity towards GCase (IC_{50} 0.1-30 μM) in this assay (less than 20% inhibition of any other of the assayed lysosomal glycosidases at 100 μM concentration).

Cell Cultures, Chaperone Tests and Toxicity Assays. Normal and Gaucher disease patients' skin fibroblasts were cultured in Dulbecco modified Eagle's medium (WAKO) supplemented with 10% fetal bovine serum (Nichirei Biosci. Inc., Tokyo, Japan) at 37 ºC in 5% CO_2. For measurement of chaperone activities, fibroblasts were plated onto 35 mm dishes at 50,000 cells per dish. After 24 h incubation, the medium with the indicated concentrations of compound was applied and cells were cultured for 96 hours. Then, the lysates in 0.1% Triton-X100/distilled H_2O were collected from the cells and assayed for lysosomal GCase as described above. To measure the cytotoxic effect of the compounds, normal human fibroblasts were plated onto 35

mm dishes at 15,000 cells per dish and incubated overnight. Then the medium was changed with or without compounds. After 24 h incubation, the supernatant of the cells was collected and measured by the lactate dehydrogenase assay (WAKO). All the cell lines used were tested for mycoplasma contamination before conducting the chaperone and toxicity assays.

Immunofluorescence Microscopy. Immunofluorescence microscopy was performed using standard methods as previously described.[40] Cover slips were analyzed using a fluorescence microscope (Leica DMRE, Leica Microsystems GmbH, Wetzlar, Germany). Deconvolution studies and 3-dimensional projections were performed using a DeltaVision system (Applied Precision, Issaquah, WA) with an Olympus IX-71microscope. The deconvolved images were derived from optical sections taken at 30-nm intervals using a 60× PLAPON objective with a 1.42 numerical aperture. More than 100 cells in 10 randomly obtained images were evaluated in each experiment to confirm reproducibility.

Docking Experiments. The structure of wild type human GCase was modeled by homology-based simulated annealing using Modeller 9v7[77] and the X-ray diffraction models of Gcase at pH 4.5 and 5.5 (pdb codes: 1OGS, 3GXM and 3GXI)[65,78] and of the partially deglycosylated enzyme at pH 6 (pdb: 2F61).[79] The RMSD value between the distinct structures were lower than 0.4 Å. MOL2 coordinate files of the chaperones were obtained with ChemOffice (PerkinElmer) and submitted to flexible docking with the enzyme using Autodock Vina[80] and monitored in UCSF Chimera.[81] Both, the ligand and protein loops were treated as flexible. The best of the 10 lowest score structures were selected in each computation, and then submitted to energy minimization and MD (20 ns MD trajectories) for further refinement. The Antechamber[82] module of Amber 14[83] was used to assign the general Amber force field parameters[84] and AM1-BCC charges[85] to the PC models. Simulations were performed under periodic boundary

conditions using orthorhombic cell geometry (the minimum distance between protein and cell faces was initially set at 10 Å) and particle mesh Ewald (PME) electrostatics with a Ewald summation cutoff of 9 Å. The structures were solvated with extended simple point charge model (SPC) water molecules,[86] and Cl^- counter-ions were added to neutralize the net charge of the full systems. Afterwards, solvent and counter-ions were subjected to 2500 steps of steepest descent minimization followed by 500 ps NPT-MD computations using isotropic molecule position scaling and a pressure relaxation time of 2 ps at 298 K. Then, energy minimization was carried out in the overall system, which was then submitted to 300 ps temperature equilibration to 298 K followed by a production run under the microcanonical ensemble. The SHAKE algorithm[87] was used to constrain bonds involving hydrogen atoms. The PTRAJ module of AMBER and LIGPLOT[88] were used for data analyses.

Statistical Analysis. All results are expressed as mean±SD of three independent experiments, each conducted in triplicate. The measurements were statistically analyzed using the Student's *t* test for comparing 2 groups. The level of significance was set at $p<0.05$.

ASSOCIATED CONTENT

Supporting Information

PDB files for the computational models obtained after docking of compound **22** and compound **11** with GCase (Figures 6 and S1), ^{1}H NMR and ^{13}C NMR spectra of all new compounds, Lineweaver-Burk plots for K_i and enzyme inhibition mode determinations, excitation spectra of pyrene in water containing increasing concentrations of the fluorinated chaperones **21**-**24** and plots for CMC determinations, ^{1}H NMR spectra of the 1:1 inclusion complexes of **21**-**24** with βCD, selected ^{1}H or ^{19}F NMR spectra from titration experiments as well as the corresponding

binding isotherm plots, and toxicity data for compounds **21**-**24** and their complexes with β-cyclodextrin in healthy human fibroblasts. This material is available free of charge via the Internet at http://pubs.acs.org.

AUTHOR INFORMATION

Corresponding Authors

*For C.O.M.: phone: +34 954559806; fax: +34 954624960; e-mail: mellet@us.es.

*For J.M.G.F.: phone: +34 954489553; fax: +34 954460161; e-mail: jogarcia@iiq.csic.es.

*For J. A. S.-C.: phone: +34 954978071; e-mail: jasanalc@upo.es.

*For K.H.: phone: +81 859 38 6472; fax: +81 859 38 6470; e-mail: kh4060@med.tottori-u.ac.jp.

Author Contributions

#These authors contributed equally.

Notes

The authors declare no competing financial interest.

ACKNOWLEDGMENTS

The Spanish Ministerio de Economía y Competitividad (MINECO; contract numbers SAF2016-76083-R, CTQ2015-64425-C2-1-R, BFU2015-71017-P and CTQ2013-43310), the Spanish Ministerio de Sanidad (contract number FIS PI13/00129), the Junta de Andalucía (contract numbers CTS-5725, FQM2012-1467 and BIO-198), the Generalitat Valenciana (PROMETEOII/2014/073), the Ministry of Education, Culture, Science, Sports and Technology of Japan (KAKENHI), the Ministry of Health, Labour and Welfare of Japan (H17-Kokoro-019, H20-Kokoro-022) and the European Union Seventh Framework Programme (FP7-People-2012-

CIG), grant agreement number 333594 (to E. M. S.-F., Marie Curie Reintegration Grant) are acknowledged. Cofinancing from the European Regional Development Funds (FEDER and FSE), is also acknowledged. K.H. was supported by Takeda Science Foundation. Technical assistance from the research support services of the University of Seville (CITIUS) is also gratefully acknowledged.

ABBREVIATIONS

GCase, β-glucocerebrosidase; GlcSph, glycosylsphingosine, psychosine; GlcCer, glucosylceramide; GD, Gaucher disease, LSD, lysosomal storage disorder, ERT, enzyme replacement therapy; SRT, substrate reduction therapy; ER, endoplasmic reticulum; ERAD, endoplasmic reticulum-associated degradation; UPR, unfolded protein response; PC, pharmacological chaperone; BBB, blood-brain barrier; βCD, β-cyclodextrin; AIJ, 1,6-anhydro-L-idonojirimycin; CMC, critical micellar concentration; β-Glcase, β-glucosidase; PDI, protein disulfide isomerase; LAMP-2, lysosome associated membrane protein 2; ESIMS: electrospray ionization mass spectrometry; FABMS, fast atom bombardment mass spectrometry; HRFABMS, high resolution fast atom bombardment mass spectrometry; TBTU, O-(benzotriazol-1-yl)-N,N,N',N'-tetramethyluronium tetrafluoroborate; DIEA, N,N,-diisopropylethylamine; NN-DNJ, *N*-nonyl-1-deoxynojirimycin.

REFERENCES

(1) Farfel-Becker, T.; Futerman, A. H. Cellular pathogenesis in sphingolipid storage disorders: the quest for new therapeutic approaches. *Clin. Lipidol.* **2010**, *5*, 255–265.

(2) Vitner, E. B., Platt, F. M.; Futerman, A. H. Common and uncommon pathogenic cascades in lysosomal storage diseases. *J. Biol. Chem.* **2010**, *285*, 20423–20427.

(3) Wennekes, T.; van den Berg, J. B. H. N.; Boot, R. G.; van der Marel, G. A.; Overkleeft, H. S.; Aerts, J. M. F. G. Glycosphingolipids—Nature, function, and pharmacological modulation *Angew. Chem. Int. Ed.* **2009**, *48*, 8848-8869.

(4) Nilsson, O.; Svennerholm, L. Accumulation of glucosylceramide and glucosylsphingosine (psychosine) in cerebrum and cerebellum in infantile and juvenile Gaucher disease. *J. Neurochem.* **1982**, *39*, 709-718.

(5) Orvisky, E.; Park, J. K.; LaMarca, M. E.; Ginns, E. I.; Martin, B. M.; Tayebi, N.; Sidransky, E. Glucosylsphingosine accumulation in tissues from patients with Gaucher disease: correlation with phenotype and genotype. *Mol. Genet. Metab.* **2002**, *76*, 262-270.

(6) Baris, H. N.; Cohen, I. J.; Mistry, P. K. Gaucher disease: the metabolic defect, pathophysiology, phenotypes and natural history. *Pediatr. Endocrinol. Rev*. **2014**, *12*, 72-81.

(7) Sidransky, E. Gaucher disease: complexity in a "simple" disorder. *Mol. Genet. Metab.* **2004**, *83*, 6-15.

(8) Oh, D.-B. Glyco-engineering strategies for the development of therapeutic enzymes with improved efficacy for the treatment of lysosomal storage diseases. *BMB Rep.* **2015**, *48*, 438-444.

(9) Scott, L. J. Eliglustat: a review in Gaucher disease type 1. *Drugs* **2015**, *75*, 1669-1678.

(10) Platt, F. M.; Jeyakumar, M. Substrate reduction therapy. *Acta Paediatr.* **2008**, *97*, 88-93.

(11) Gupta, N.; Oppenheim, I.M.; Kauvar, E.F.; Tayebi, N.; Sidransky, E. Type 2 Gaucher disease: phenotypic variation and genotypic heterogeneity. *Blood Cells Mol. Dis.* **2011**, *46*, 75-84.

(12) Vembar, S. S.; Brodsky, J. L. One step at a time: endoplasmic reticulum-associated degradation. *Nat. Rev. Mol. Cell Biol.* **2008**, *9*, 944-957.

(13) Yang, C.; Swallows, C. L.; Zhang, C.; Lu, J.; Xiao, H.; Brady, R. O.; Zhuang, Z. Celastrol increases glucocerebrosidase activity in Gaucher disease by modulating molecular chaperones. *Proc. Natl. Acad. Sci. U. S. A.* **2014**, *111*, 249-254.

(14) Ingemann, L.; Kirkegaard, T. Lysosomal storage diseases and the heat shock response: convergences and therapeutic opportunities. *J. Lipid Res.* **2014**, *55*, 2198-2210.

(15) Jian, J.; Zhao, S.; Tian, Q.-Y.; Liu, H.; Zhao, Y.; Chen, W.-C., Grunig, G.; Torres, P. A.; Wang, B. C.; Zeng, B.; Pastores, G.; Tang, W.; Sune, Y.; Grabowski, G. A.; Kong, M. X.; Wang, G.; Chen, Y.; Liang, F.; Overkleeft, H. S.; Saunders-Pullman, R.; Gerald L. Chan, G. L.; Liu, C. Association between progranulin and Gaucher disease. *EBioMedicine* **2016**, *11*, 127-137.

(16) Parenti, G.; Andria, G.; Valenzano, K. J. Pharmacological chaperone therapy: preclinical development, clinical translation, and prospects for the treatment of lysosomal storage disorders. *Mol. Ther.* **2015**, *23*, 1138-1148.

(17) Boyd, R. E.; Lee, G.; Rybczynski, P.; Benjamin, E. R.; Khanna, R.; Wustman, B. A.; Valenzano, K. J. Pharmacological chaperones as therapeutics for lysosomal storage diseases. *J. Med. Chem.* **2013**, *56*, 2705-2730.

(18) Benito, J. M.; García Fernández, J. M.; Ortiz Mellet, C. Pharmacological chaperone therapy for Gaucher disease: a patent review. *Expert Opin. Ther. Pat.* **2011**, *21*, 885-903.

(19) Sánchez-Fernández, E. M.; García Fernández, J. M.; Ortiz Mellet, C. Glycomimetic-based pharmacological chaperones for lysosomal storage disorders: lessons from Gaucher, G_{M1}-gangliosidosis and Fabry diseases. *Chem. Commun.* **2016**, *52*, 5497-5515.

(20) Brumshtein, B.; Greenblatt, H. M.; Butters, T. D.; Shaatiel, Y.; Aviezer, D.; Silman, I.; Futerman, A. H.; Sussman, J. L. Crystal structures of complexes of N-butyl- and N-nonyl-deoxynojirimycin bound to acid β-glucosidase: insights into the mechanism of chemical chaperone action in Gaucher disease. *J. Biol. Chem*. **2007**, *282*, 29052-29058.

(21) Compain, P.; Martin, O. R.; Boucheron, C.; Godin, G.; Yu, L.; Ikeda K.; Asano, N. Design and synthesis of highly potent and selective pharmacological chaperones for the treatment of Gaucher's disease. *ChemBioChem* **2006**, *7*, 1356-1359.

(22) Lin, H.; Sugimoto, Y.; Ohsaki, Y.; Ninomiya, H.; Oka, A.; Taniguchi, M.; Ida, H.; Eto, Y.; Ogawa, S.; Matsuzaki, Y.; Sawa, M.; Inoue, T.; Higaki, K.; Nanba, E.; Ohno, K.; Y. Suzuki. *N*-Octyl-β-valienamine up-regulates activity of F213I mutant β-glucosidase in cultured cells: a potential chemical chaperone therapy for Gaucher disease. *Biochim. Biophys. Acta* **2004**, *1689*, 219-228.

(23) Trapero, A.; Alfonso, I.; Butters, T. D.; Llebaria, A. Polyhydroxylated bicyclic isoureas and guanidines are potent glucocerebrosidase inhibitors and nanomolar enzyme activity enhancers in Gaucher cells. *J. Am. Chem. Soc*. **2011**, *133*, 5474-5484.

(24) Castilla, J.; Rísquez, R.; Cruz, D.; Higaki, K.; Nanba, E.; Ohno, K.; Suzuki, Y.; Díaz, Y.; Ortiz Mellet, C.; García Fernández, J. M.; Castillón, S. Conformationally-Locked *N*-Glycosides with Selective β-Glucosidase Inhibitory Activity: Identification of a new non-iminosugar-type pharmacological chaperone for Gaucher disease. *J. Med. Chem*. **2012**, *55*, 6857-6865.

(25) Castilla, J.; Rísquez, R.; Higaki, K.; Nanba, E.; Ohno, K.; Suzuki, Y.; Díaz, Y.; Ortiz Mellet, C.; García Fernández, J. M.; Castillón, S. Conformationally-locked *N*-glycosides: Exploiting long-range nonglycone interactions in the design of pharmacological chaperones for Gaucher disease. *Eur. J. Med. Chem*. **2015**, *90*, 258-266.

(26) Navo, C. D.; Corzana, F.; Sánchez-Fernández, E. M.; Busto, J. H.; Avenoza, A.; Zurbano, M. M.; Nanba, E.; Higaki, K.; Ortiz Mellet, C.; García Fernández, J. M.; Peregrina, J. M. Conformationally-locked *C*-glycosides: tuning aglycone interactions for optimal chaperone behaviour in Gaucher fibroblasts. *Org. Biomol. Chem.* **2016**, *14*, 1473-1484.

(27) Maegawa, G. H. B.; Tropak, M. B.; Buttner, J. D.; Rigat, B. A.; Fuller, M.; Pandit, D.; Tang, L.; Kornhaber, G. J.; Hamuro, Y.; Clarke, J. T.; Mahuran, D. J. identification and characterization of ambroxol as an enzyme enhancement agent for Gaucher disease. *J. Biol. Chem.* **2009**, *284*, 23502-23516.

(28) Patnaik, S.; Zheng, W.; Choi, J. H.; Motabar, O.; Southall, N.; Westbroek, W.; Lea, W. A.; Velayati, A.; Goldin, E.; Sidransky, E.; Leister, W.; Marugan, J. J. Discovery, structure-activity relationship, and biological evaluation of noninhibitory small molecule chaperones of glucocerebrosidase. *J. Med. Chem.* **2012**, *55*, 5734-5748.

(29) Goddard-Borger, E. D.; Tropak, M. B.; Yonekawa, S.; Tysoe, C.; Mahuran, D. J.; Withers, S. G. Rapid assembly of a library of lipophilic iminosugars via the thiol–ene reaction yields promising pharmacological chaperones for the treatment of Gaucher disease. *J. Med. Chem.* **2012**, *55*, 2737-2745.

(30) Mena-Barragán, T.; Narita, A.; Matias, D.; Tiscornia, G.; Nanba, E.; Ohno, K.; Suzuki, Y.; Higaki, K.; García Fernández, J. M.; Ortiz Mellet, C. pH-Responsive pharmacological chaperones for rescuing mutant glycosidases. *Angew. Chem. Int. Ed.* **2015**, *54*, 11696-11700.

(31) García-Moreno, M. I.; Díaz-Pérez, P.; Ortiz Mellet, C.; García Fernández, J. M. Castanospermine−trehazolin hybrids: a new family of glycomimetics with tuneable glycosidase inhibitory properties. *Chem. Commun.* **2002**, 848-849.

(32) Luan, Z.; Higaki, K.; Aguilar-Moncayo, M.; Ninomiya, H.; Ohno, K.; García-Moreno, M. I.; Ortiz Mellet, C.; García Fernández, J. M.; Suzuki, Y. Chaperone activity of bicyclic nojirimycin analogues for Gaucher mutations in comparison with *N*-(*n*-nonyl)deoxynojirimycin. *ChemBioChem* **2009**, *10*, 2780-2792.

(33) Luan, Z.; Higaki, K.; Aguilar-Moncayo, M.; Li, L.; Ninomiya, H.; Namba, E.; Ohno, K.; García-Moreno, M. I.; Ortiz Mellet, C.; García Fernández, J. M.; Suzuki, Y. Fluorescent sp^2-iminosugar with pharmacological chaperone activity for Gaucher disease: synthesis and intracellular distribution studies. *ChemBioChem* **2010**, *11*, 2453-2464.

(34) Tiscornia, G.; Lorenzo Vivas, E.; Matalonga, L.; Berniakovich, I.; Barragán Monasterio, M.; Argaiz, C. E.; Gort, L.; González, F.; Ortiz Mellet, C.; García Fernández, J. M.; Ribes, A. Veiga, A.; Izpisua Belmonte, J. C. Neuronopathic Gaucher's disease: induced pluripotent stem cells for disease modelling and testing chaperone activity of small compounds. *Hum. Mol. Genet.* **2013**, *22*, 633-645.

(35) Brumshtein, B.; Aguilar-Moncayo, M.; García-Moreno, M. I.; Ortiz Mellet, C.; García Fernández, J. M.; Silman, I.; Shaaltiel, Y.; Aviezer, D.; Sussman, J. L.; Futerman, A. H. 6-Amino-6-deoxy-5,6-di-*N*-(*N'*-octyliminomethylidene)nojirimycin: synthesis, biological

evaluation, and crystal structure in complex with acid β-glucosidase. *ChemBioChem* **2009**, *10*, 1480-1485.

(36) Brumshtein, B.; Aguilar-Moncayo, M.; Benito, J. M.; García Fernández, J. M.; Silman, I.; Shaaltiel, Y.; Aviezer, D.; Sussman, J. L.; Futerman, A. H.; Ortiz Mellet, C. Cyclodextrin-mediated crystallization of acid β-glucosidase in complex with amphiphilic bicyclic nojirimycin analogues. *Org. Biomol. Chem.* **2011**, *9*, 4160-4167.

(37) García-Moreno, M. I.; Ortiz Mellet, C.; García Fernández, J. M. Synthesis of calystegine B_2, B_3, and B_4 analogues: Mapping the structure-glycosidase inhibitory activity relationships in the 1-deoxy-6-oxacalystegine series. *Eur. J. Org. Chem.* **2004**, 1803-1819.

(38) Aguilar-Moncayo, M.; Gloster, T. M.; García- Moreno, M. I.; Ortiz Mellet, C.; Davies, G. J.; Llebaria, A.; Casas, J.; Egido-Gabás, M.; García Fernández, J. M. Molecular basis for β-glucosidase Inhibition by ring-modified calystegine analogues. *ChemBioChem* **2008**, *9*, 2612-2618.

(39) Alfonso, P.; Andreu, V.; Pino-Angeles, A.; Moya-García, A. A.; García-Moreno, M . I.; Rodríguez-Rey, J. C.; Sánchez-Jiménez, F.; Pocoví, M.; Ortiz Mellet, C.; García Fernández, J. M.; Giraldo P. Bicyclic derivatives of L-idonojirimycin as pharmacological chaperones for neuronopathic forms of Gaucher disease. *ChemBioChem* **2013**, *14***,** 943-949.

(40) de la Mata, M.; Cotán, D.; Oropesa-Avila, M.; Garrido-Maraver, J.; Cordero, M. D.; Villanueva Paz, M.; Delgado Pavón, A.; Alcocer-Gómez, E.; de Lavera, I.; Ybot-González, P.; Zaderenko, A. P.; Ortiz Mellet, C.; García Fernández, J. M.; Sánchez-Alcázar, J. A. Pharmacological chaperones and coenzyme Q_{10} treatment improves mutant β-glucocerebrosidase

activity and mitocondrial function in neuronopathic forms of Gaucher disease. *Sci. Rep.* **2015**, *5*, 10903.

(41) Chang, H.-H.; Asano, N.; S. Ishii, S.; Ichikawa, Y.; Fan, J.-Q. Hydrophilic iminosugar active-site-specific chaperones increase residual glucocerebrosidase activity in fibroblasts from Gaucher patients. *FEBS J.* **2006**, *273*, 4082-4092.

(42) Kato, A.; Nakagome, I.; Nakagawa, S.; Koike, Y.; Nash, R. J.; Adachi, I.; Hirono, S. Docking and SAR studies of calystegines: Binding orientation and influence on pharmacological chaperone effects for Gaucher's disease. *Bioorg. Med. Chem.*, **2014**, *22*, 2435-2441.

(43) Yu, Y.; Mena-Barragán, T.; Higaki, K.; Johnson, J. L.; Drury, J. E.; Lieberman, R. L.; Nakasone, N.; Ninomiya, H.; Tsukimura, T.; Sakuraba, H.; Suzuki, Y.; Namba, E.; Ortiz Mellet, C.; García Fernández, J. M.; Ohno, K. Molecular basis of 1-deoxygalactonojirimycin arylthiourea binding to human α-galactosidase A: pharmacological chaperoning efficacy on Fabry disease mutants. *ACS Chem. Biol.* **2014**, *9*, 1460-1469.

(44) García-Moreno, M. I.; Benito, J. M.; Ortiz Mellet, C.; García Fernández. Synthesis and evaluation of calystegine B_2 analogues as glycosidase inhibitors. *J. Org. Chem.* **2001**, *66*, 7604-7614.

(45) Gillis, E. P.; Eastman, K. J.; Hill, M. D.; Donnelly, D. J.; Meanwell, N. A. Applications of fluorine in medicinal chemistry. *J. Med. Chem.* **2015**, *58*, 8315-8359.

(46) Bassetto, M.; Ferla, S.; Pertusati, F. Polyfluorinated groups in medicinal chemistry. *Future Med. Chem.* **2015**, *7*, 527-546.

(47) Schitter, G.; Steiner, A. J.; Pototschnig, G.; Scheucher, E.; Thonhofer, M.; Tarling, C. A.; Withers, S. G.; Fantur, K.; Paschke, E.; Mahuran, D. J.; A. Rigat, B. A.; Tropak, M. B.; Illaszewicz, C.; Saf, R.; Stütz, A. E.; Wrodnigg, T. M. Fluorous iminoalditols: a new family of glycosidase inhibitors and pharmacological chaperones. *ChemBioChem* **2010**, *11*, 2026-2033.

(48) Fantur, K. M.; Wrodnigg, T. M.; Stütz, A. E.; Pabst, B. M.; Paschke, E. Fluorous iminoalditols act as effective pharmacological chaperones against gene products from *GLB1* alleles causing G_{M1}-gangliosidosis and Morquio B disease. *J. Inherited Metab. Dis.* **2012**, *35*, 495-503.

(49) Le Guen, C.; Mena-Barragán, T.; Ortiz Mellet, C.; Gueyrad, D.; Pfund, E.; Lequeux, T. Fluorinated hydroxypiperidines as selective β-glucosidase inhibitors. *Org. Biomol. Chem.* **2015**, *13*, 5983-5996.

(50) Park, K.; Kitteringham, N. R.; O'Neill, P. M. Metabolism of fluorine-containing drugs. *Annu. Rev. Pharmacol. Toxicol.* **2001**, *41*, 443-4470.

(51) Palchevskyy, S. S.; Posokhov, Y.O.; Olivier, B.; Popot, J.-L.; Pucci, B.; Ladokhin, A.S. Chaperoning of membrane protein insertion into lipid bilayers by hemifluorinated surfactants: application to diphtheria toxin. *Biochemistry* **2006**, *45*, 2629-2635.

(52) Abellán Flos, M.; García Moreno, M. I.; Ortiz Mellet, C.; García Fernández, J. M. Nierengarten, J.-F.; Vincent, S. P. Potent glycosidase inhibition with heterovalent fullerenes: unveiling the binding modes triggering multivalent inhibition. *Chem. Eur. J.* **2016**, *22*, 11450-11460.

(53) Compain, P.; Bodlenner, A. The multivalent effect in glycosidase inhibition: A new, rapidly emerging topic in glycoscience. *ChemBioChem* **2014**, *15*, 1239-1251.

(54) Karoyo, A. H.; Borisov, A. S.; Wilson, L. D.; Hazendonk, P. Formation of host-guest complexes of β-cyclodextrin and perfluorooctanoic acid. *J. Phys. Chem. B* **2011**, *115*, 9511-9527.

(55) Xing, H.; Lin, S.-S.; Yan, P.; Xiao, J.-X. Demicellization of a mixture of cationic-anionic hydrogenated/fluorinated surfactants through selective inclusion by α- and β-cyclodextrin. *Langmuir* **2008**, *24*, 10654-10664.

(56) Vecsernyés, M.; Fenyvesi, F.; Bácskay, I.; Deli, M. A.; Szente, L.; Fenyvesi, E. Cyclodextrins, blood-brain barrier, and treatment of neurological diseases. *Arch. Med. Res.* **2014**, *45*, 711-729.

(57) Tiwari, G.; Tiwari, R.; K. Rai, A. Cyclodextrins in delivery systems: applications. *J. Pharm. Bioallied Sci.* **2010**, *2*, 72-79.

(58) Popot, J.-L. Amphipols, nanodiscs, and fluorinated surfactants: three nonconventional approaches to studying membrane proteins in aqueous solutions. *Annu. Rev. Biochem.* **2010**, *79*, 737-775.

(59) Dax, K.; Gaigg, B.; V. Grassberger, V.; Kölblinger, B.; Stütz, A. E. Einfache Synthesen von 1,5-Didesoxy-1,5-imino-D-glucit (1-Desoxynojirimycin) und 1,6-Didesoxy-1,6-imino-D-glucit aus D-Glucofuranurono-6,3-lacton. *J. Carbohydr. Chem.* **1990**, *9*, 479-499.

(60) Wilhelm, M.; Zhao, C. L.; Wang, Y.; Xu, R.; Winnik, M. A.; Mura, J. L.; Riess, G.; Croucher, M. D. Poly(styrene-ethylene oxide) block copolymer micelle formation in water: a fluorescence probe study. *Macromolecules* **1991**, *24*, 1033-1040.

(61) Takai, T.; Higaki, K.; Aguilar-Moncayo, M.; Mena-Barragán, T.; Hirano, Y.; Yura, K.; Yu, L.; Ninomiya, H.; García-Moreno, M.I.; Sakakibara, Y.; Ohno, K.; Nanba, E.; Ortiz Mellet, C.; García Fernández, J. M.; Suzuki, Y. A bicyclic 1-deoxygalactonojirimycin derivative as a novel pharmacological chaperone for G_{M1} gangliosidosis. *Mol. Ther.* **2013**, *21*, 526-532.

(62) Bisson, A. P.; Carver, F. J.; Eggleston, D. S.; Haltiwanger, R. C.; Hunter, C. A.; Livingston, D. L.; McCabe, J. F.; Rotger, C.; Rowan, A. E. Synthesis and recognition properties of aromatic amide oligomers: molecular zippers. *J. Am. Chem. Soc.* **2000**, *122*, 8856-8868.

(63) Rodríguez-Lavado, J.; de la Mata, M.; Jiménez-Blanco, J. L; García-Moreno, M. I.; Benito, J. M.; Díaz-Quintana, A.; Sánchez-Alcázar, J. A.; Higaki, K.; Nanba, E.; Ohno, K.; Suzuki, Y.; Ortiz Mellet, C.; García Fernández, J. M. Targeted delivery of pharmacological chaperones for Gaucher disease to macrophages by a mannosylated cyclodextrin carrier. *Org. Biomol. Chem.* **2014**, 12, 2289-2301.

(64) T. Mena-Barragán, García-Moreno, M. I.; Nanba, E.; Higaki, K.; Concia, A. L.; Clapés, P.; García Fernández, J. M.; Ortiz Mellet, C. Inhibitor versus chaperone behaviour of D-fagomine, DAB and LAB sp^2-iminosugar conjugates against glycosidases: a structure-activity relationship study in Gaucher fibroblasts. *Eur. J. Med. Chem.* **2016**, *121*, 880-891.

(65) Wei, R. R.; Hughes, H.; Boucher, S.; Bird, J. J.; Guziewics, N.; Van Patten, S. M.; Qiu, H.; Pan, C. Q.; Edmunds, T. X-ray and biochemical analysis of N370S mutant human acid β-glucosidase. *J. Biol. Chem.* **2011**, 286, 299-308.

(66) Dvir, H.; Harel, M.; McCarthy, A. A.; Toker, L.; Silman, I.; Futerman, A. H.; Sussman, J. L. X-ray structure of human acid-β-glucosidase, the defective enzyme in Gaucher disease. *EMBO Rep.*, **2003**, *4*, 704-709.

(67) Bendikov-Bar, I.; Maor, G.; Filocamo, M.; Horowitz, M. Ambroxol as a pharmacological chaperone for mutant glucocerebrosidase. *Blood Cells Mol. Dis.* **2013**, *50*, 141-145.

(68) Sawkar, A. R.; Adamski-Werner, S. L.; Cheng, W.-C.; Wong, C.-H.; Beutler, E.; Zimmer, K.-P.; Kelly, J. W. Gaucher disease-associated glucocerebrosidases show mutation-dependent chemical chaperoning profiles. *Chem. Biol.* **2005**, *12*, 1235-1244.

(69) Sawkar, A. R.; Cheng, W.-C.; Beutler, E.; Wong, C.-H.; Balch, W. E.; Kelly, J. W. Chemical chaperones increase the cellular activity of N370S β-glucosidase: a therapeutic strategy for Gaucher disease. *Proc. Natl. Acad. Sci. U. S. A.* **2002**, *99*, 15428-15433.

(70) Yadav, A. K.; Shen, D. L.; Shan, X.; He, X.; Kermode, A. R.; Vocadlo, D. J. Fluorescence-quenched substrates for live cell imaging of human glucocerebrosidase activity. *J. Am. Chem. Soc.* **2015**, *137*, 1181-1189.

(71) Sidransky, E.; Nalls, M. A.; Aasly, J.O.; Aharon-Peretz, J.; Annesi, G. Barbosa, E. R.; Bar-Shira, A; Berg, D.; Bras, J.; Brice, A.; Chen, C. M.; Clark, L. N.; Condroyer, C.; De Marco, E. V.; Dürr, A.; Eblan, M. J.; Fahn, S.; Farrer, M. J.; Fung, H. C.; Gan-Or, Z.; Gasser, T.; Gershoni-Baruch, R.; Giladi, N.; Griffith, A.; Gurevich, T.; Januario, C.; Kropp, P.; Lang, A. E.; Lee-Chen, G.-J.; Lesage, S.; Marder, K.; Mata, I.F.; Mirelman, A.; Mitsui, J.; Mizuta, I.; Nicoletti, G.; Oliveira, C.; Ottman, R.; Orr-Urtreger, A.; Pereira, L. V.; Quattrone, A.; Rogaeva, E.; Rolfs, A.; Rosenbaum, H.; Rozenberg, R.; Samii, A.; Samaddar, T.; Schulte, C.; Sharma, M.; Singleton, A.; Spitz, M.; Tan, E.-K.; Tayebi, N.; Toda, T.; Troiano, A. R.; Tsuji, S.; Wittstock,

M.; Wolfsberg, T.G.; Wu, Y.-R.; Zabetian, C. P.; Zhao, Y.; Ziegler, S.G. Multicenter analysis of glucocerebrosidase mutations in Parkinson's disease. *N. Engl. J. Med.* **2009**, *361*, 1651-1661.

(72) Migdalska-Richards, A.; Schapira, A. H. V. The relationship between glucocerebrosidase mutations and Parkinson disease. *J. Neurochem.* **2016**, *139* (Suppl. 1), 77-90.

(73) Schapira, A. H. V. Glucocerebrosidase and Parkinson disease: recent advances. *Mol. Cell. Neurosci.* **2015**, *66*, 37-42.

(74) Mazzulli, J. R.; Zunke, F.; Tsunemi,T.; Toker, N. J.; Jeon, S.; Burbulla, L. F.; Patnaik, S.; Sidransky, E.; Marugan, J. J.; Sue, C. M.; Krainc, D. Activation of β-glucocerebrosidase reduces pathological α-synuclein and restores lysosomal function in Parkinson's patient midbrain neurons. *J. Neurosci.* **2016**, *36*, 7693-7706.

(75) Dardonville, C.; Fernández-Fernández, C.; Gibbons, S-L.; Ryan, G. J.; Jagerovic, N.; Gabilondo, A. M.; Meana, J. J.; Callado, L. F. Synthesis and pharmacological studies of new hybrid derivatives of fentanyl active at the μ-opioid receptor and I_2–imidazoline binding sites *Bioorg. Med. Chem.* **2006**, *14*, 6570-6580.

(76) Bisson, A. P.; Hunter, C. A.; Morales, J. C.; Young, K. Cooperative interactions in a ternary mixture. *Chem. Eur. J.* **1998**, *4*, 845-851.

(77) Eswar, N.; Eramian, D.; Webb, B.; Shen, M.-Y; Sali, A. Protein structure modeling with MODELLER. *Methods Mol. Biol.* **2008**, *426*, 145-159.

(78) Lieberman, R. L.; D'aquino, J. A.; Ringe, D.; Petsko, G. A. Effects of pH and iminosugar pharmacological chaperones on lysosomal glycosidase structure and stability, *Biochemistry* **2009**, *48*, 4816-4827.

(79) Liou, B., Kazimierczuk, A.; Zhang, M., Scott, C. R.; Hegde, R. S.; Grabowski, G. A. Analyses of variant acid β-glucosidases: effects of Gaucher disease mutations, *J. Biol. Chem.* **2006**, *281*, 4242-4253.

(80) Trott, O.; Olson, A. J. AutoDock Vina: improving the speed and accuracy of docking with a new scoring function, efficient optimization, and multithreading. *J. Comput.Chem.* **2010**, *31*, 455-461.

(81) Pettersen, E. F.; Goddard, T.D.; Huang, C.C.; Couch, G.S.; Greenblatt, D.M;, Meng, E.C.; Ferrin, T.E. UCSF Chimera - a visualization system for exploratory research and analysis. *J. Comput. Chem.* **2004**, *25*, 1605-1612.

(82) Wang, J.; Wang, W.; Kollman, P. A.; Case, D. A. Automatic atom type and bond type perception in molecular mechanical calculations. *J. Mol. Graphics Modell.* **2006**, *25*, 247-260.

(83) Case, D. A.; Babin, V.; Berryman, J. T.; Betz, R. M.; Cai, Q.; Cerutti, D. S.; Cheatham, III, T. E.; Darden, T. A.; Duke, R. E.; Gohlke, H.; Goetz, A. W.; Gusarov, S.; Homeyer, N.; Janowski, P.; Kaus, J.; Kolossváry, I.; Kovalenko, A.; Lee, T. S.; LeGrand, S.; Luchko, T.; Luo, R.; Madej, B.; Merz, K. M.; Paesani, F.; Roe, D. R.; Roitberg, A.; Sagui, C.; Salomon-Ferrer, R.; Seabra, G.; Simmerling, C. L.; Smith, W.; Swails, J.; Walker, R. C.; Wang, J.; Wolf, R. M.; Wu, X.; Kollman, P. A. *AMBER 14*; University of California: San Francisco, CA, **2014**.

(84) Wang, J.; Wolf, R. M.; Caldwell, J. W., Kollman, P. A.; Case, D. A. Development and testing of a general amber force field, *J. Comput. Chem.* **2004**, *25*, 1157-1174.

(85) Jakalian, A.; Jack, D. B.; Bayly, C. I. Fast, efficient generation of high-quality atomic charges. AM1-BCC model: II. Parametrization and validation. *J. Comput. Chem.* **2002**, *23*, 1623-1641.

(86) Berendsen H. J. C.; Postma J. P. M.; van Gunsteren W. F.; Hermans J. Interaction models for water in relation to protein hydration. In *Intermolecular Forces*; Pullmann, B., Ed.; Reidel: Dordrecht, **1981**; pp. 331-342.

(87) Ryckaert, J. P.; Ciccotti, G.; Berendsen, H. J. C. Numerical-integration of cartesian equations of motion of a system with constraints – molecular dynamics of N-alkanes, *J. Comput. Phys.* **1977**, *23*, 327-341.

(88) Wallace, A. C.; Laskowski, R. A.; Thornton, J. M. LIGPLOT: a program to generate schematic diagrams of protein-ligand interactions, *Protein Eng.* **1995**, *8*, 127-134.

For Table of Contents Only